IAEA-TECDOC-1481

Anthropogenic analogues for geological disposal of high level and long lived waste

Final report of a coordinated research project 1999–2004

IAEA
International Atomic Energy Agency

December 2005

IAEA-TECDOC-1481

Anthropogenic analogues for geological disposal of high level and long lived waste

Final report of a coordinated research project 1999–2004

IAEA
International Atomic Energy Agency

December 2005

The originating Section of this publication in the IAEA was:

Waste Technology Section
International Atomic Energy Agency
Wagramer Strasse 5
P.O. Box 100
A-1400 Vienna, Austria

ANTHROPOGENIC ANALOGUES FOR GEOLOGICAL DISPOSAL OF HIGH LEVEL AND LONG LIVED WASTE
IAEA, VIENNA, 2005
IAEA-TECDOC-1481
ISBN 92–0–113105–4
ISSN 1011–4289

Printed by the IAEA in Austria
December 2005

FOREWORD

The long term safety of a disposal facility depends on the performance of the whole multibarrier system. It comprises both engineered, human-made elements and natural barriers: the host rock formation and the surrounding geological environment. While the long term development of the geological environment has been studied worldwide and is well understood and reasonably predictable, information is rather limited on the behaviour of human-made materials during time periods comparable with the required duration of their functioning as part of the barrier system.

Human-made barriers of a geological repository include the waste form (mostly vitrified and ceramic materials); waste packaging consisting of different metals and alloys; sealing, buffering and plugging materials made preferably of modified natural raw materials. Also, construction materials (concrete based, metals) may be left underground when closing the facility and, even if they have not been designed to provide a long term safety function, they may influence repository behaviour.

To predict and validate by experimental evidence the long term functioning of engineered barriers some Member States have carried out studies on archaeological and anthropogenic objects allowing estimation of the nature and rate of degradation processes affecting their longevity. In 1999, the IAEA initiated the Coordinated Research Project (CRP) on Anthropogenic Analogues for Geological Disposal of High Level and Long Lived Radioactive Waste with the intention of supporting this effort. It was intended to gather the results of national projects aiming at the characterization of human-made materials exposed for a long time to conditions similar to those of disposal and to link the laboratories carrying out these studies.

This publication gives a short overview of recent developments in anthropogenic analogue studies and summarizes the five year effort of several laboratories. Their individual results are presented in detail in the annexes. The IAEA wishes to thank all those who participated in this CRP and contributed to this publication.

The text was finalized with the assistance of N. Chapman, Switzerland. The IAEA officers responsible for the CRP and this publication were M. Raynal, M. Knapp, J.-M. Potier and L. Nachmilner of the Division of Nuclear Fuel Cycle and Waste Technology.

EDITORIAL NOTE

CONTENTS

1. INTRODUCTION

1.1. Background

Human-made materials comprise important elements of the engineered barriers within the multi-barrier containment system in all concepts for the geological disposal of long lived radioactive wastes. A typical waste package consists of a metallic container for the solid waste (e.g. spent fuel or borosilicate glass in the case of high level waste, or cemented intermediate level wastes), possibly with an additional metallic over-pack to provide added protection or further corrosion resistance to the container. In the repository, waste packages are surrounded by buffer or backfill materials, such as clays, which have been subject to varying degrees of mechanical or chemical processing. Repository concepts for intermediate level wastes generally contain large volumes of cement and concrete in various applications: as a waste conditioning matrix, in boxes for waste components, as backfill between waste packages and as vault and silo structures within excavated caverns and tunnels.

The long term behaviour and interactions of these materials is an important aspect of the performance of a repository, and post-closure safety assessment requires information on their durability, stability and slow degradation characteristics. While some of this information comes from thermodynamic models and normal or accelerated material testing procedures, the very long timescales involved in repository evolution mean that information on the preservation of analogous, ancient archaeological materials can provide extremely valuable supporting evidence. Analogue information from archaeological and other anthropogenic materials can indicate the mechanisms and rates of long term corrosion of glasses and metals and of degradation of cements over hundreds or thousands of years, which can be used to constrain estimates of degradation rates over similar or longer periods. Under some circumstances it is also possible to find these materials in locations where they have interacted with natural radionuclides over long periods. This can provide useful data on how radionuclides might be sorbed or precipitated as they pass from the waste matrix into the surrounding, degrading engineered barrier system of a repository far into the future.

Much archaeological material has survived in conditions that are more aggressive or dynamic than those that would be encountered in a deep repository — typically, conditions in the soil may be more oxidising and there is likely to be more organic material present and, therefore, more active biological degradation processes. Consequently, although the direct analogy with repository conditions may be weak, much archaeological analogue information tends to provide usefully conservative values of degradation rates. Nevertheless, the preservation of ancient artefacts, often in very good condition, from as much as 3000-4000 years ago can give considerable confidence in the value of an engineered barrier system and provide useful qualitative indicators to explain disposal concepts to the public.

Over the last twenty five years, many countries have gathered information on the preservation of archaeological materials — typically copper, bronze and iron objects, glasses, cements and ceramics — all of which have analogues in waste disposal systems. Numerous studies have been carried out and there is an extensive pool of information from different countries, different historical epochs and different preservation environments (see [1–4] for recent compilations). The present report contributes to this growing database by presenting scoping studies on materials from several geographical regions which have so far been poorly represented in this field of study, namely China, Eastern Europe and South America. Much interest has frequently been expressed in the potential of materials from the historical development of these regions to provide useful analogue data that extends the scope of earlier studies.

The studies reported are mainly concerned with metals, glasses and cements and are largely exploratory in nature. The results support the findings of similar, earlier evaluations in other countries (mainly Europe) and add to the growing database on rates of metal and glass corrosion and on cement-radionuclide interactions.

This TECDOC thus represents a contribution to the information base on archaeological analogues, with emphasis on ancient copper-based materials and glasses. It is expected that it will provide other workers in the field with an insight into the characteristics of materials from the four countries studied and promote further cooperation in the future.

1.2. Objectives

The purpose of the coordinated research project (CRP) was to enhance understanding of the long term behaviour of the geologic disposal system. Specifically, this project was initiated to find out to what extent anthropogenic analogues could provide scientific information and data to support the geological disposal option, its concepts and employment of different barrier materials.

1.3. Scope

The report addresses the performance of human-made items exposed to the natural conditions. The selection of materials includes cement, glass, and metallic objects of variable age ranging from tens to more than three thousand years. The focus of the report is on methods employed in characterization of selected samples and on understanding and quantification of degradation processes appearing in the studied, mostly geochemical, systems.

1.4. Structure

The report consists of two main parts: (i) background information about the anthropogenic analogue issue and a short review of existing studies on similar archaeological materials and (ii) an Annex containing summaries of the individual country projects. Specifically, corrosion of copper based metals, mainly bronzes, was studied (Argentina, China, Ukraine), short and long term performance of glass in contact with soils was characterized (Czech Republic, Ukraine), and mineralogical development of concrete and its interactions with radioactive water were evaluated (Czech Republic).

2. ARCHAEOLOGICAL ANALOGUES OF METALS

Metals play an important role in the engineered barrier systems of all repository designs for long lived waste disposal. They will be used in:

- Canisters and overpacks for vitrified high level waste and spent fuel;
- Containers for solidified and compacted intermediate level waste (ILW);
- Reinforced concrete structures such as vaults and silos in ILW repositories;
- Rock support and reinforcement systems (bolts, nets, anchors, liners) in most geological environments.

Interest in the longevity of metals is primarily concerned with waste containers and overpacks. Recognition of their long term corrosion behaviour is of cardinal importance for understanding and quantitative description of degradation processes. The main consideration is given to the following aspects:

- Rates of uniform corrosion;
- Pitting and stress corrosion enhancement;
- Corrosion products (properties and evolution with time).

Only a few of the metals being considered for waste containers are represented in historical materials. These are iron and steel, copper and bronze. Clearly, ‘exotic’ metals, for example, Ti or the Ni-Cr-Mo alloys are to be used in the US spent fuel repository, and stainless steels (Fe-Cr-Ni alloys) cannot be studied using archaeological analogues. As usually found in analogue studies, even for those materials we have at our disposal, the analogies are not perfect. Ancient steel is compositionally different from modern steels and most copper-containing artefacts are bronzes (copper-tin alloys) rather than the pure copper being developed for spent fuel containers.

Safety assessments of repository systems that use wholly iron or steel containers generally assume only limited lifetimes and make conservative assumptions of hundreds to a few thousand years before containment within the canister/overpack is lost. Copper containers are expected to retain their integrity for very much longer — tens of thousands of years. Nevertheless, for both materials there has been equal interest in finding ancient analogues that have survived in environments comparable to disposal systems for thousands of years.

Although it is useful to be able to use analogues to scope laboratory-derived corrosion rate data for both iron and copper, the ambition level for iron analogues has been more limited. Because container lifetime is in any case assumed to be short, some investigation programmes have shown that large masses of iron degrade slowly whilst retaining their structural form and that the corrosion products offer some measure of protection to iron at the core of the mass (e.g. as found in the famous seven tonne hoard of Roman nails and other iron objects buried in a shallow pit at the legionary fortress of Inchtuthil in Scotland [5]).

Archaeological artefacts made from smelted iron date back almost 4000 years – a period of time at least four times longer than that commonly assumed for the functioning of iron and steel waste containers. Bronze artefacts date back somewhat further in time, although this is still short compared to the design basis lifetime of copper containers for spent fuel.

The compilation of corrosion rate data developed by Johnson and Francis [6] still remains the most comprehensive information on both iron and copper artefacts from a range of preservation environments, although it has been supplemented by several more recent studies. By examining archaeological artefacts from museum collections, they were able to constrain uniform corrosion rates of iron and iron alloys to 0.1 to 10 μm/a and copper and copper alloys to 0.025 to 1.27 μm/a with an average of about 0.3 μm/a. A parallel study by Tylecote [7] investigated in more detail at the soil chemistry of sites from which copper and bronze artefacts had been recovered and concluded that 0.225 μm/a was the average rate, with tin-bronzes being the most corrosion resistant material.

These magnitudes of uniform corrosion rate suggest that a massive iron container for long lived wastes might last for ~100 000 years [8], but the iron artefacts provide little or no information on enhanced corrosion by pitting, which would reduce this lifetime significantly. Studies of pitting in copper and bronze artefacts give average values of around three for the pitting factor — much lower than had been assumed in early safety assessments.

The relevance of using museum specimens is often challenged, as these have usually undergone exceptional level of preservation — highly corroded materials never find their way into museum exhibits (although they may be kept among the records of excavations). However, given that almost all archaeological material has been preserved in soils within a few metres of Earth's surface it must be assumed that even exceptionally preserved material has experienced at least some period of relatively dynamic hydrochemical conditions, compared to those of a deeply buried waste container surrounded by an impermeable clay buffer. Waste containers would be expected to fare better than almost all archaeological materials[1], so it is reasonable to assume that average corrosion data from artefacts from a range of preservation environments represent an upper boundary on those for waste containers in a chemically unperturbed engineered barrier system.

Nevertheless, the number of analogue studies of metallic artefacts is very limited. Those that have been published in the last twenty-five years are listed in Table I.

Given the general sparsity of analogues of metallic artefacts, the usefulness of new studies, especially of materials with good provenance that permit access to related soils and other materials from the same preservation environment is clear. There are also compositional differences in bronzes from different continents which may help to extend the information base. For example, ancient bronzes from South America tend to be richer in As, Ni and Zn than those from Europe, reflecting compositional differences in ore provenance.

In this respect, the present IAEA study has regarded metals of variable composition from new regions. Results gained have contributed to extending the current technical knowledge and, thus, provided additional inputs for selecting container materials suitable for particular geological disposal system.

TABLE I. OVERVIEW OF RECENTLY PUBLISHED ANALOGUE STUDIES OF METALLIC ARTEFACTS

Metal	Subject	Ref.
Iron and steel	Corrosion rate estimates from 40 iron and iron alloy artefacts	[6]
	More than one million Roman nails from the Inchtuthil iron hoard, Scotland (dating from 87 AD)	[9]
	Buried steel gas and water pipes	[10]
	1600 year old iron pillar in Delhi, India. Passivating corrosion layer of crystalline iron hydrogen phosphate hydrate, amorphous iron oxyhydroxides and magnetite.	[11]
Copper and bronze	Corrosion rate estimates from 34 archaeological artefacts	[6]
	Impact of preservation chemical environment on corrosion rates of artefacts from 53 sites	[7]
	Pitting factors for copper and copper alloys from Bronze Age, Roman and more recent artefacts	[12], [13]
	Copper cannon from the 17th century Swedish warship Kronan, preserved partly in seabed mud and partly directly exposed to seawater	[14], [15]
	3600 year-old bronze artefacts buried in volcanic ash from the eruption of the Santorini volcano, Greece. It was possible to study the movement of leached copper in the soil floors immediately beneath the artefacts.	[16]

---

[1] Especially if they are in a chemically reducing and alkaline environment (as when surrounded by cement and concrete) — in such conditions steel is expected to have a very long lifetime as a result of the formation of a passivating layer of magnetite.

3. ARCHAEOLOGICAL ANALOGUES OF GLASS

Vitrified high level waste uses a predominantly borosilicate glass matrix composition for the waste radionuclides. In safety assessment studies, the interest is in finding analogous materials that will provide data on the long term degradation rate and mechanisms of glass under disposal conditions. This process starts once the glass has been contacted by groundwater after its container has corroded. The factors that are of value in performance assessment modelling are:

— Rate of release of radionuclides as a function of time after exposure to groundwater;
— The structure and impact on subsequent glass leaching of the gel alteration layer that forms on the glass surface;
— The potential secondary retention properties of glass alteration products;
— The effect of radiation on the above mechanisms.

Much of the analogue data on glass comes from natural (basaltic) silicate glasses, even though they are compositionally somewhat different. The only direct analogues of borosilicate glasses are from historical materials. The earliest, archaeological glasses date back as far as 4500 years and have subsequently being developed across a wide range of compositions, commonly being soda-lime or potash-lime formulations [17], again compositionally dissimilar to HLW glass.

Despite the fragility of glass objects and the metastable nature of all glasses, archaeological artefacts have survived intact for as long as 3500 years [18]. Many have experienced surface alteration (crizzling, pitting, crusting and formation of mineral films) by exposure to water either in soil or in the atmosphere.

Uranium glasses (the subject of the Czech study reported here) have been manufactured since the early 1800s [19], especially in Bohemia, and became popular owing to their strong yellow or green colouration, caused by the incorporation of uranium, or uranium and copper, into the glass. They provide the opportunity to look both at radiation effects and, for buried glass items, at uranium leaching behaviour in the ground. However, prior to the current IAEA project, no analogue studies were known to have been attempted on these materials [2].

4. ARCHAEOLOGICAL ANALOGUES OF CEMENTS

Cement and concrete will almost certainly be used in some manner in all types of deep geological repository. For most low and intermediate level waste repository design concepts, concrete is an integral structural component of the engineered barrier system, in the form of vaults and silos, or boxes for waste containers. In addition, cement-based backfills and grouts would fill void space in such designs. Cementitious material can comprise up to 90% of the total mass of materials emplaced in a repository [20]. The hyperalkaline conditions within cement-based engineered barriers mean that many radionuclides will have low solubilities and the cement gel and minerals would provide large surface areas for sorption. Owing to the highly alkaline nature of water in contact with cement, which may adversely affect clay-based buffers, its use as structural material in high level waste repository designs is avoided, although its use as rock grout and support is probably unavoidable in parts of a repository away from waste emplacement areas.

In this context, the main issues of interest in design and safety assessment are:

- The durability of the cement and the longevity of its hyperalkaline and low hydraulic conductivity conditions;
- Interactions with surrounding rock, affecting their containment properties;
- Production of colloids in cement barriers;
- Ability to sorb radionuclides.

In the present project, only the last two topics have been studied.

There are numerous examples of cements and concrete in the archaeological record. Prior to the early 19th century, mainly lime-based cements were in the use. The Romans discovered that the addition of pozzuolanic materials allowed cements to be used in underwater construction. Portland cement has been used for almost 150 years and is the type of cement that would most likely be used in a waste repository.

Archaeological analogue studies have looked at both ancient lime-based cement structures, mainly from the viewpoint of durability, and at Portland cement structures, to evaluate the longer term development of the calcium silicate hydrate phases as the cement and concrete matures [2]. No archaeological analogue studies are known that have looked at the interactions of natural radionuclides with old cements, as carried out in the present work. The most closely related study to that described here, although only in terms of material and environment, was an evaluation of leaching of cement from a 90 year old water tank in Sweden [21].

5. MATERIALS IN THE PRESENT STUDY

The current document has put together information on a range of materials from four countries that have not previously been involved in anthropogenic analogue studies for radioactive waste disposal. The investigated materials are shown in Table II.

A common aspect of most of the metal objects evaluated is that, like those from earlier studies, it was generally not possible to make direct studies of their immediate preservation environment. With the exception of the Ukrainian glass samples (which were collected specifically for the purposes of this project, along with samples of related soils), all these samples were museum specimens. However, it was possible to compile information about typical soil conditions and climate in each area, which gave some idea of the chemical environment in which the artefacts survived prior to excavation. The Chinese bronze artefacts were all castings. They had not been cleaned after excavation and some still retained soil adhered to their surfaces. The material from Argentina was all hand forged and annealed, not cast, and came from excavations carried out between about 1900 and 1988. It again appeared not to have been cleaned mechanically or chemically after discovery. The Ukrainian artefacts were both simple casts and casts with subsequent thermal and mechanical working.

The tin bronze objects from Argentina, China and the Ukraine covered a wide range of compositions, containing between 63–95 wt% Cu and 4–25 wt% Sn. The Argentinean materials included a Cu-Zn (~2:1) alloy bell, a Cu-Zn (~4:1) alloy nail, and a Cu (91 wt%) – Pb (5 wt%) alloy ship's hull plate recovered from a river bed. Some of the Ukrainian and Chinese artefacts also contained up to 4 wt% Pb.

In addition to bronze artefacts, several pure copper artefacts (with minor admixtures of Al, Ag, Mg, Si, Sn and Pb) were excavated from one site in the Ukraine.

The uranium glass samples were taken from a depth of about 0.5 to 2 m in a partially eroded landfill at an old glass factory site at Klastersky Mlyn in the Czech Republic. They typically contained about 0.1–0.4 wt% U and were of an alkali (Na, K)-calcium silicate type. The landfill is in the unsaturated zone but is believed to have been flooded periodically as it lies near a river. Leaching of glass under oxidising conditions has led to localised concentrations of U in the upper 2 m of soil in the landfill.

TABLE II. MATERIALS TESTED WITHIN THE CRP

Country	Materials studied	Age (years BP)
Argentina	Bronze chisels Bronze knife and plate Bronze bell and bracelet Copper ship's hull cladding and nail	800 550 1030 176
Czech Republic	Uranium glass from glass manufacturing waste landfill Concrete from basins used to collect high natural radioactivity waters in a deep mine	~80 ~10 and ~80
China	Bronze artefacts from Zhou and Shang dynasty tombs Bronze artefacts from Han dynasty tombs	3000–3300 1800
Ukraine	Glass Bronze arrows, ring, plate and coin Pure copper nail, wire and plate (all from the ancient Black Sea area settlements of Kamenka and Olbiya)	1700–1900 2100–2400 2400–3000

The Ukrainian glasses were small fragments of colourless to blue tableware from the 2nd and 3rd century AD, showing different degrees of corrosion, indicated by silvery films on their surface and/or by bright iridescent colours. All samples were collected from the same soil horizon, along with samples of the soil.

The concrete samples were obtained from water collection basins (100–300 m^3) in the disused Svornost mine near Jachymov in the Czech Republic. Since 1924 two of the basins were used to collect high natural series groundwater from depths of 100 to 500 m. The water was pumped to the surface for the use in local spas. The third basin was utilised for less than 10 years. Samples were taken by drilling into the walls and floor of the basins. Concrete from the older two basins contained a basaltic gravel component, while the concrete from the third one was filled by quartz sand and gravel. Both concres were highly porous (~20%). Unfortunately, it only proved possible to carry out limited studies of this material in the project.

6. SUMMARY OF KEY FINDINGS

The studies examined the thickness and nature of the alteration layer on the corroded metal objects and on glass fragments, and allowed to drew conclusions on mechanisms and rates of uniform corrosion. The principle findings of the studies can be summarised as follows:

— The Chinese bronze samples from archaeological sites in semi-tropical humid regions exhibited corrosion crusts of 320–800 μm compared to 50–260 μm measured for samples from sites in drier, temperate climate zone. A maximum corrosion rate of about

0.27 µm/a was estimated, which was close to the average values of Tylecote and Johnson/Francis [6–7] (see Figure 1).

- The Argentinean bronzes spanned a greater range of corrosion rates. The five artefacts for which rates could be estimated with high certainty (Group 1 in Figure 1) were within the range 0.08 to 0.17 µm/a. Those with high uncertainty (from the La Paya site — Group 2 in Figure 1) could have a maximum rate an order of magnitude higher (up to about 2.5 µm/a). The Group 1 values were within the range observed by Johnson and Francis [6]. No pitting corrosion was observed on any of the bronze samples.
- Corrosion rates for the 2100–2400 year old bronzes from the Ukraine were related to their Sn content (see Figure 1) and they are in a similar range to the other materials reported in this project, with maximum values somewhat greater than the Johnson and Francis control set. High Sn bronzes had the lowest corrosion rates, which were of an order of magnitude lower than the typical rate of an atmospheric corrosion of a modern tin bronze. However, they were subject to brittle mechanical failure. One artefact made of low Sn bronze that had been thermally and mechanically worked after casting had an equivalently low corrosion rate.
- Corrosion of bronzes mobilised Cu from the metal, forming a passivating corrosion crust. In the Chinese bronzes, this comprised an inner layer of red oxide overlain by an outer carbonate (malachite) layer, with associated minor oxide, carbonate and hydroxide phases of Sn, Cu and Pb. The two sites studied in the Ukraine had different soils, with those containing higher levels of organic matter, S and Cl and with a higher pH being the most aggressive with respect to corrosion.
- Pure copper artefacts from the Ukraine displayed an outer rim of cuprite, malachite, and covellite mineralization, incorporating Cl, C, Fe and Al from the surrounding soils. Simple cast samples had larger and less homogeneous grain sizes compared to thermally and mechanically worked – forged – castings and were prone to corrosion penetration along grain boundaries. Corrosion rates for worked copper are in the lower end of the overall range for bronzes (see Figure 1). A cast copper artefact had a higher corrosion rate, near the upper end of the range given by Johnson and Francis.
- Corrosion of the uranium glass samples was uniform, resulting in an altered layer between 100–500 µm thick with a sharp interface with the unaltered glass and no transition zone. Leaching removed Na, K and U preferentially, leading to a relative increase in Si and Ca concentration in the alteration layer. There were indications that uranium might then be re-concentrated at the outer surface of the alteration layer. The estimated corrosion rate was 1.25–6.25 µm/a.
- The 80-year old glass samples contained bubbles and were generally inhomogeneous. The origin of the bubbles was not clear. They might be air from the manufacturing process or helium/radon accumulations.
- The composition of several 10s to 100s µm thick, structurally complex surface layer on corroded glass from the Ukraine revealed that the larger cations (Na, Ca and, partially, Si) had been leached out, while Al was accumulated in the degraded surface layer – characteristic for processes of weathering of silicates and aluminosilicates. Compositional differences in the glasses mean that a range of corrosion behaviour can be seen in different samples from the same preservation environment. Samples

containing inclusions of organic substances indicated the highest degree of alteration/decay, but the role of organic matter in this process is not clear.

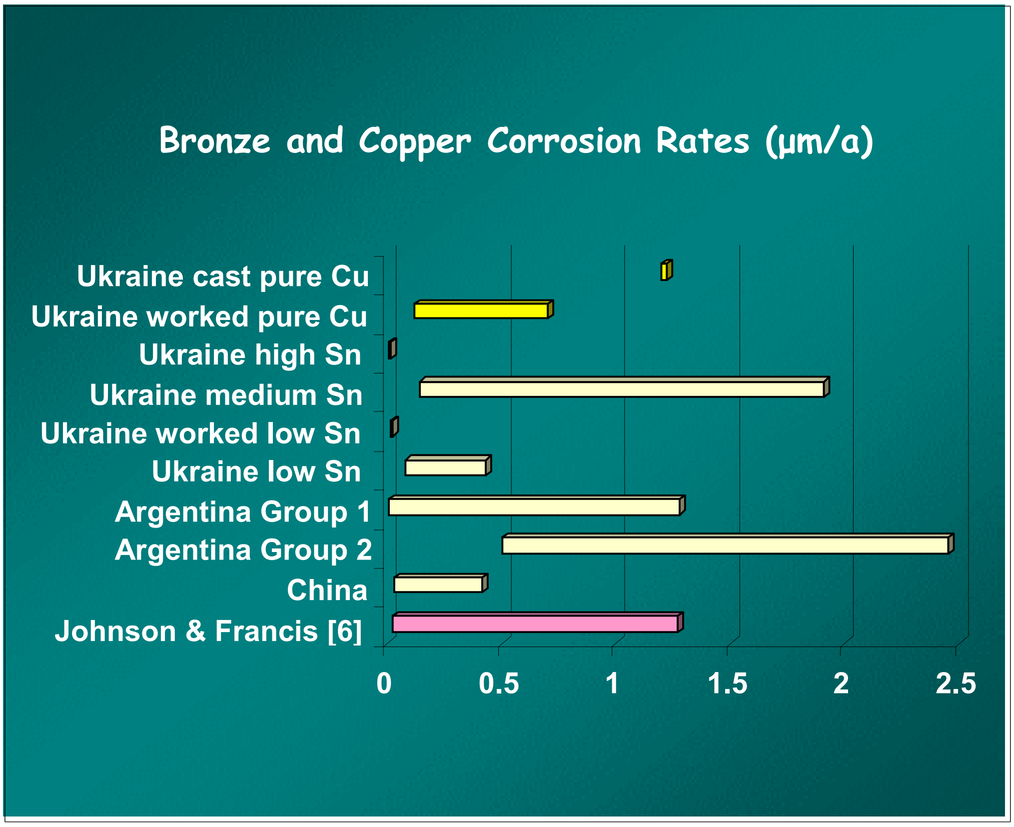

FIG. 1. Comparison of ranges of bronze and copper corrosion rates from this study with those of copper and bronze artefacts reported by Johnson and Francis [6].

***Note**: Argentina Group 1 was the material from the Tilcara and Elordi sites and the ship's copper plate from the River Plate, which had low measurement uncertainty ranges (<0.1 μm/a). Argentina Group 2 was the material from the La Paya site, with greater measurement uncertainty (up to 0.9 μm/a). The ranges of Sn concentrations for the Ukrainian samples were: low was 2 to 4 wt%; medium was 11 to 17 wt%; high was 23 to 25 wt%.*

— The two concrete samples of different age (80 and 10 years) that were studied showed clear differences in the hardened cement matrix. Crystalline phases (ettringite, portlandite) in the younger concrete were partially replaced by more stable phases like smectite or zeolites. Despite cement aging and phase transformation, both concrete samples retained high pH buffering capacity, as shown in leaching tests. The low measured concentration of U and Th indicated low mobility of these elements in the hyperalkaline environment.

The detailed outcomes of the particular projects can be found in the Annexes to this report. The key results mentioned above support, in particular, the general conclusions on longevity of metal containers and vitrified HLW materials that have been drawn from previous studies of similar materials from Europe.

There is clearly scope for more detailed evaluation of some of the material that has emerged in this study. An overall conclusion that has been stated in earlier reviews listed in references is that it would be most useful to be able to analyse material as it is excavated, allowing direct observations of the preservation environment and interactions of the artefacts with their matrix. This would be a useful primary objective for any further investigations.

REFERENCES

[1] MILLER, W.M., CHAPMAN, N.A., Postcards from the Past: Archaeological and Industrial Analogues for Deep Repository Materials, Radwaste Magazine, 2, 32 (1995).

[2] MILLER, W., ALEXANDER, R., CHAPMAN, N.A., MCKINLEY, I., SMELLIE, J., Geological Disposal of Radioactive Wastes and Natural Analogues, Pergamon Press, 316 (2000).

[3] STUCKLESS, J.S., Archaeological Analogues for Assessing the Long-Term Performance of a Mined Geologic Repository for High level Radioactive Waste, Open-File Report 00-181, Denver, Colorado: U.S. Geological Survey. ACC: MOL.20000822.0366 (2000).

[4] CRWMS, Natural Analogue Synthesis Report. USDOE Civilian Radioactive Waste Management System, Management and Operating Contractor Report TDR-NBS-GS-000027 REV00 ICN 02 (2002).

[5] ANGUS, N.S., BROWN, G.T., CLEERE, H.F., The Iron Nails from the Roman Legionary Fortress at Inchtuthil, Perthsire, J. Iron and Steel Institute, 200, 956 (1962).

[6] JOHNSON, A.B., FRANCIS, B., Durability of Metals from Archaeological Objects, Metal Meteorites and Native Metals, Batelle Pacific Northwest Laboratories Report No. PNL-3198 (1980).

[7] TYLECOTE, R.F., The Effect of Soil Conditions on the Long-term Corrosion of Buried Tin-bronzes and Copper, J. Archaeological Science, 6, 3435 (1979).

[8] ALEXANDER, W.F., McKINLEY, I.G., A Review of the Application of Natural Analogues in Performance Assessment: Improving Models of Radionuclide Transport in Groundwaters, J. Geochemical Exploration, 46, 83 (1992).

[9] PITTS, L., ST. JOSEPH, A., Inchtuthil Roman Legionary Fortress Excavation 1952–1965, Allan Sutton (1985).

[10] YUSA, Y., KAMEI, G., ARAI, T., Some Aspects of Natural Analogue Studies for Assessment of Long-term Durability of Engineered Barrier Materials – Recent Activities at PNC Tokai, Japan, In: Natural Analogues Working Group Fourth Meeting Report, B. Côme and N.A. Chapman (Eds.), CEC report 13014, 215 (1991).

[11] BALASUBRAMANIAM, R., On the Corrosion Resistance of the Delhi Iron Pillar, Corrosion Science, 42, 2103, Elsevier, TIC: 251551 (2000).

[12] BRESLE, A., SAERS, J., ARRHENIUS, B., Studies in Pitting Corrosion on Archaeological Bronzes, SKB Technical Report TR 83-05, SKB Stockholm, Sweden (1983).

[13] MATTSSON, E., Corrosion Resistance of a Copper Canister for Spent Nuclear Fuel, SKB Technical Report 83-24, SKB, Stockholm, Sweden (1983).

[14] HALLBERG, R.O., ÖSTLUND, P., WADSTEN, T., A 17th Century Bronze Cannon as Analogue for Radioactive Waste Disposal, In: Natural analogues in radioactive waste disposal, B. Côme and N.A. Chapman (Eds.), CEC report 11037 EN, Graham and Trotman, 135 (1987).

[15] NERETNIEKS, I., Investigations of Old Bronze Cannons, In: Natural Analogues Working Group Second Meeting Report, B. Côme and N.A. Chapman (Eds.), CEC report 10671, 191 (1986).

[16] MURPHY, W.M., PEARCY, E.C., GREEN, R.T., PRIKRYL, J.D., MOHANTY, S., LESLIE, B.W., NEDUNGADI, A., A Test of Long-term, Predictive Geochemical Transport Modelling at the Akrotiri Archaeological Site, J. Contaminant Hydrology, 29, 245 (1998).

[17] VANDIVER, P.B., Corrosion of Synthesised Glasses and Glazes as Analogues for Nuclear Waste Degradation, Materials Research Society Symposium Proceedings, 333, Scientific Basis for Radioactive Waste Management XVII, 969 (1994).

[18] KAPLAN, M.F., An Archaeological Perspective on a Modern Issue: Nuclear Waste Disposal, J. Field Archaeology, 7 (1980) 265.

[19] TOMABECHI, K. Uranium Glass, Iwanami Book Service Centre, Tokyo (1995).

[20] ALEXANDER, W.F., Natural Cements: How Can They Help us Safely Dispose of Radioactive Waste? Radwaste Magazine, September 1995, 62, American Nuclear Society (1995).

[21] TRÄGÅRDH, J., LAGERBLAD, B., Leaching of 90 Year Old Concrete Mortar in Contact with Stagnant Water, SKB Technical Report TR 98-11, SKB, Stockholm, Sweden (1998).

ANNEX A

ARGENTINA

STUDIES ON THE BEHAVIOUR OF ANCIENT MAN-MADE MATERIALS AS ANALOGUES OF MATERIALS USED FOR THE DISPOSAL OF HIGH-ACTIVITY AND LONG LIVED WASTE

T.A. Palacios[1], E.D. Cabanillas[1,2], C. Semino[1], L.R. González[3]
[1] Comisión Nacional de Energía Atómica, Buenos Aires, Argentina
[2] CONICET, Buenos Aires, Argentina
[3] Museo Etnográfico, Universidad Nacional de Buenos Aires, Argentina

Abstract

The disposal of high-activity and long lived waste (HLW) requires the study of ancient materials distinguished by their longevity in different environments in order to predict the long-term durability of the waste containers. The patina thickness of pre-Columbian and historical artefacts from Argentina was measured and their corrosion rates determined. The results can be used as an example of the durability of some man-made materials for designing HLW repositories.

1. INTRODUCTION

Ancient human-made materials may yield useful information on the behaviour and longevity of engineered barriers for the disposal of radioactive waste. To assess confidence in the models and data used in the design of disposal systems it is necessary to use information drawn from studies of natural and anthropogenic systems that may be similar to those that will occur in repositories. These anthropogenic analogues include all kinds of archaeological and historical metal artefacts, including meteoritic iron and native metals. To understand the durability of materials it is necessary to perform studies of degradation mechanisms such as oxidation, corrosion, embrittlement, etc.

This work presents examples of the longevity of different copper based alloys found in Argentina, South America. A collection of pre-Columbian and historical bronzes studied from the Rio de la Plata (River Plate) and the northwest part of Argentina, as examples of degradation of metals owing to corrosion.

Copper has an impressive corrosion resistance and, for this reason, is nowadays chosen for applications where the environment is aggressive (condensers, plumbing, roofing, coinage, cookware, etc.). Besides the native copper that has been on our planet for millions of years, it is well known that man-made copper and its alloy artefacts have survived for millennia in natural environments. Hundreds of thousands of metallic objects still exist in good condition, many of them found by archaeologists.

Many of the properties of copper are important, and its low corrosion rate is the reason why it is chosen for HLW containers. The corrosion rate of the metal must take into consideration the design of the container wall. Copper corrosion layers are formed relatively fast during the first decades of contact with the normal environment – after that the rate of corrosion decreases. Many authors have studied man-made analogues in order to assess the long-term corrosion behaviour of copper and, in particular, ancient bronze and other copper base alloys [1]. Modern experiments have been reported by Uhlig [2] on average atmospheric copper corrosion over periods of 8 to 20 years. Swedish researchers studied the bronze Kronan cannon because it was considered a good example of the resistance of copper alloys to corrosion. This canon was buried at the bottom of the Baltic Sea in 1676. The cannon was protected by the sea bottom clay from the corrosive action of oxygen dissolved in seawater. Nevertheless, a complex redox equilibrium is established between the Cu^{2+} from tenorite inclusions in the cannon and Fe and organic matter in the clay. It developed a corrosion layer of 0.8 mm thickness [3–4].

Robbiola et al. [1] studied a group of 28 pieces of bronze selected from a collection of Bronze Age metallurgical centre in Fort-Harrouard, France. They proposed two classes of corrosion structures. Type I structure is defined as a two-layer passivity deposit due to internal oxidation with a decuprification process (i.e. selective dissolution of copper). Type II structure corresponds to more severe attacks, such as pitting, but also general uneven corrosion, and is modelled by a three-layer structure, characterized by the presence of cuprous oxide and by an increase in the chloride content at the patina/alloy interface, related to selective dissolution of copper.

Another study was made on a collection of Swedish Bronze Age objects that had been exposed to near-surface burial conditions for periods of up to 3000 years. The objects would have been exposed to water with low chloride and high bicarbonate, continuously aerated, which increases the susceptibility to pitting. Furthermore the presence of inclusions and alloying elements and crude metallurgical procedures may have rendered the objects more susceptible to pitting than modern oxygen-free Cu alloys [5].

Johnson and Francis presented a set of 36 artefacts made of copper and copper alloys from different regions, registering the minimum and maximum estimated corrosion rates [6].

In this work, a set of archaeological artefacts was selected of similar metallurgical characteristics. All objects were hand forged and annealed, with equiaxial grains and annealed twins and we have studied the composition of the alloys and the thickness of natural patina of ancient copper based alloys. The growth of corrosion patinas and corrosion rates were measured considering the different conditions such as alloy composition, characteristics of the environments (soil and water) and different ages (in soil or water and in museums). The patina thickness was determined in relation to the elapsed time.

The study was focused on the corrosion rates of archaeological and historical bronzes artefacts of this part of South America, considering the different environmental conditions of northwest Argentina. This region has different natural conditions compared to the Old World, with dissimilar weathering conditions, geological events, contamination types and different technologies of ancient civilizations.

Metallurgy started in ancient times in two different regions, independently of each other. The oldest was in the Near East, 10000 years ago, and from that region it extended to Europe and the Far East and Africa. The other started in the Central Andean region in 1500 BC, extending from the north and south of the Andes to the rest of the Americas. More than 3500 years before that time, the Old Copper Culture developed near the Great Lakes in North America, with no significant technological relevance. Both metallurgies were similar but delayed in time. They started using native metals, such as gold, silver and copper (platinum in South America) and afterwards they introduced bronzes, firstly arsenical bronzes and later, tin bronzes. The great difference is that the Near East developed iron metallurgy whereas, in the America, this metal was not known. On the other hand, the Americas employed platinum metal, which was unknown in Europe and Asia until the discovery of America by the Europeans. The small difference between the Old World and the New World bronzes was in chemical compositions, perhaps due to ore compositions of their particular regions (i.e. arsenical bronzes with nickel in Bolivia, or tin bronzes with zinc in NW Argentina).

2. LOCATION OF THE STUDY

The archaeological artefacts chosen (see Table A–I) were bronze chisels from Tilcara (Jujuy Province, Northwestern Argentine), a bronze plate and a knife from La Paya (Salta Province) and a bronze fragment of a tiny bell and a fragment of a bracelet from Elordi (Salta Province). Historical artefacts were also studied. We selected a small piece of the copper alloy plate which covered the wooden hull of a ship, the frigate *25 de Mayo*, sunk at the River Plate (Rio de la Plata) in 1827, close to Buenos Aires; and a nail that fixed the plates, see Figures A–1 and A–2.

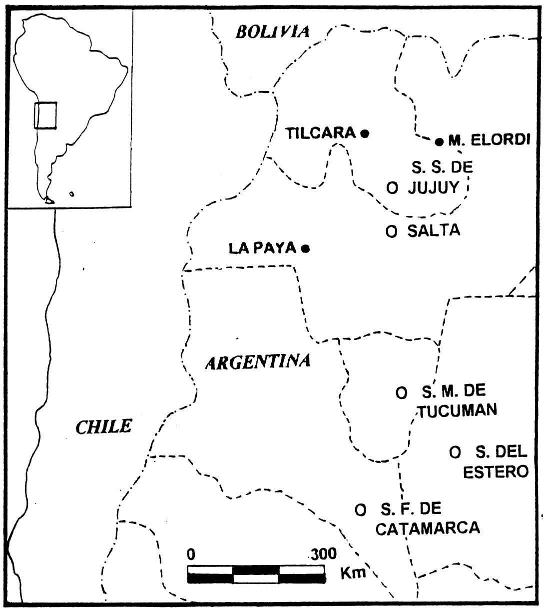

FIG. A-1: Archaeological sites.

FIG. A-2: Frigate 25 de Mayo sunken site.

The Tilcara settlement was developed from the tenth century until the Spanish conquest, before which it had been dominated by the Inca Empire [9–10]. The studied materials came from excavations done by M. Tarragó in 1988; the altitude of the site is 1470 m. The investigations allowed dating with ^{14}C, which placed the context at 800 ± 40 years before present (BP). The site comprises domestic buildings and workshops. Between the objects discovered there were combustion structures and evidence of meat consumption and cooking, fragmented ceramic of different types, deposits of clay for pottery, stone artefacts for copper mineral milling, slags, metallurgical refractories and seven metal objects, such as the four chisels selected for this study.

The La Paya objects come from excavated burials made by J. B. Ambrosetti, and published in 1907 [7–8]. La Paya is a settlement with hundreds of stone constructions made and inhabited from the X to XVII century, when the region was definitively dominated by the Europeans. In the mid-XV century it was integrated with the Inca Empire and La Paya was occupied by their officers. The evidence of the occupation consists of buildings and materials, such as metals with Inca features. Ambrosetti excavated hundreds of tombs and recovered metal objects belonging to local development times as well as to the Inca period. The funeral offerings included pottery, stone, shells and wood objects.

TABLE A–I. ARCHAEOLOGICAL AND HISTORICAL ARTEFACTS FROM ARGENTINA

Sample	Artefact	Site	Age (BP)	Cu (%)	Sn (%)	As (%)	Others
1	Chisel	Tilcara	800	85.41	12.87	—	Fe, Si, Al, Ca, Cl, As
2	Chisel	Tilcara	800	90.25	9.02	0.30	Fe, Si, Al, Ca, Cl
3	Chisel	Tilcara	800	92.20	7.44	0.38	Fe, Si, Al, Ca, Cl
4	Chisel	Tilcara	800	92.09	6.76	1.14	Fe, Si, Al, Ca, Cl
5	Plate	La Paya	550	92.11	7.60	0.27	Fe, Si, Al, Ca, Cl
6	Knife	La Paya	550	88.61	4.86	1.25	Fe, Pb, Zn, O
7	Bracelet	Elordi	1030	88.50	1.35	2.21	Fe, Pb, Zn, O
8	Bell (fragment)	Elordi	1030	65.57	0.006	0.102	Zn=31,94%, Fe, Pb, O
9	Hull	River Plate	>176	90.91	0.01	1.4	Pb=4.6%,Fe, Zn, O
10	Nail ship	River Plate	>176	76.9	0.03	0.3	Zn=18.9%, Fe, Zn, O

Tilcara and La Paya are situated in Humahuaca (Jujuy province) and in North Calchaquí Valley (Salta province), respectively, at a mean altitude of 1500 to 1800 meters. There are two geographical regions where the environment is arid, with annual rainfall less than 200 mm, concentrated in summer months. The dominant vegetation is covered with xerophilous plants and cacti. The soils are light on the surface, neutral or alkaline, with little organic material and nitrogen, moderate calcium content and average content of phosphorous, potassium and magnesium, its humidity increases with the depth.

The cemetery of Elordi was partially excavated by O. Menghin in the early 1970s and ten years later by B. Ventura [11–12], who obtained ^{14}C dates of 1030 ± 120 BP [9]. The objects studied come from the excavations and formed part of funerary offerings. The other materials were ceramic fragments, neck beads of sodalite turquoise, chrysocolle and textiles. Elordi is a burial place, near Orán in the Salta province, at the foot of the hills at 650 meters above sea level. The environment corresponds to the phytogeographical province called the Western Forest. The environmental conditions correlate with subtropical weather, with precipitation of 1000 mm per year, largely in the summer. The soils are acid with little humidity. The predominant vegetation consists of tall trees. For religious reasons, all the ancient cultures in this part of America established their cemeteries at the highest part of a site, free from flooding, and the objects from Tilcara, La Paya and Elordi come from sealed tombs.

The frigate *25 de Mayo* was seriously damaged in a sea battle, returned to the port for repair and, after a major storm, sank, close to Buenos Aires city, in 1827. She was buried in mud at the bottom of the river and was rediscovered in 1933. At this time, part of the hull, wood and metals were recovered and taken to the Naval Museum.

All the pieces studied in this project were taken from museums and they were excavated by archaeologists. The pieces were not modified since discovery — no traces of mechanical or chemical treatment were found on their surfaces. The objects from Tilcara and La Paya came from the Ethnographic Museum of Buenos Aires University and were found in archaeological excavations made by archaeologists from the Institution. The objects from

Elordi were stored in the Prehistoric Section of the Institute of Anthropological Sciences of the University of Buenos Aires and were also found by archaeologists from this Institution.

The archaeological surrounding deposits could be considered stable and without important perturbations in all the three sites. In La Paya, the materials were recovered from a sealed environment where they were preserved from degradation processes. Ambrosetti recovered wood objects, which are usually the first to disappear as a result of environmental degradation. In the Tilcara case, the excavation reports focus in detail on the insignificant degradation of the archaeological deposits by vegetable roots and rodents. Although the Elordi zone, at first sight, should have been of the worst environmental conditions for materials conservation, as a result of the sealed context within which the objects were found, textiles were recovered, which are normally the most rapidly affected after burial.

3. MATERIAL STUDIED

Samples 1 to 4 from Tilcara are small tools and, according to their shape, archaeologists call them chisels. Sample 5 is a small plate with suspension holes and sample 6 is a highly corroded knife. Sample 7 is a fragment of a bracelet and sample 8 is a fragment of a tiny bell. Sample 9 is a piece of a plate that was recovered with the wooden hull of the ship and sample 10 is a nail that fixed the plates onto the hull. All of them were corroded and their dimensions and weights are shown in Table A–II.

Small parts of each sample were cut and mounted in acrylic for metallographic preparation. After the metallographic studies, the samples were coated with a thin gold layer for analysis in the electron microprobe. The same preparation was used for the scanning electron microscopy observations. No other materials were sampled, because all the samples belong to museums.

TABLE A–II. ARCHAEOLOGICAL AND HISTORICAL ARTEFACT DIMENSIONS

Sample	**Length** (mm)	**Width** (mm)	**Thickness** (mm)	**Weight** (g)
1	44.5	10.5	4.0	5.1
2	82.2	18.2	2.5	12.3
3	63.6	9.6	1.8	5.2
4	122.5	13.6	3.0	15.0
5	69	61	5	69.8
6	118	118	2.5	76.13
7	–	–	–	7.4
8	–	–	–	1.04
9	70	70	0.3	14.4
10	40	4	4	5.7

4. ANALYTICAL METHODS

The analytical technique used was the electron microprobe (CAMECA SX 50). The electron beam used had energy of 20 kV and 30 nA current intensity. The data obtained with wavelength dispersive spectrometers were automatically corrected by the ZAF method. For the metallographic studies and measuring patina thickness we used a metallographic optical microscopy (Olympus BX60M) with a 10X objective and a 10X ocular. For the observations of patinas we used a scanning electron microscopy (Phillips PS 500 with EDAX facility).

The archaeological dating of metal artefacts was done indirectly, through other materials found in the same context (bones and other organic materials) using the ^{14}C method. We also employed information from archaeological reports. Dating of the historical artefacts was based on historical sources.

5. RESULTS

The project aimed at determinating the thickness of the archaeological bronze patinas. Samples that were buried in soils had an average patina thickness between 64 and 904 µm and those sunk in river water had the thickness between 61 and 113 µm. The corrosion rates were calculated as indicated in Table A–III.

TABLE A–III. AVERAGE THICKNESS OF PATINAS AND CORROSION RATES

Sample	**Patina thickness** (µm)	**Age** (a)	**Corrosion rate** (µm/a)
1	904	800	1.13
2	64	800	0.08
3	144	800	0.18
4	119	800	0.15
5	445	550	0.81
6	896	550	1.63
7	137	1030	0.13
8	180	1030	0.17
9	61	176*	0.34
10	113	176*	0.64

* since the ship sank

Robbiola [1] affirmed that in currently performed laboratory tests the corrosion rate is about 0.05 to 4 µm /a, in archaeological pieces the patina thickness is between 10 to 250 µm and in corrosive conditions the rates is about 36 µm/a. Metal-patina interphase elemental cross section analysis, also performed by the electron probe microanalyzer, and the elemental profiles were recorded — see Figures A–3 and A–4.

6. DISCUSSION

At the examined set of samples different behaviours of patinas were observed. This effect might be a consequence of a decrease in the amount of copper and an increase of the amount of tin, as an indication of the formation of sub-layers in the patina where a diffusion process occurs. Another consideration to take into account is the formation of cracks and holes during corrosion (see Figure A–5). Based on the metallographic and microprobe investigations of the bronze artefacts we can conclude that corrosion was preferably inter-granular: no pitting corrosion was identified (see Figure A–6).

It is remarkable that the corrosion was only partly dependent on the kind of soils and surroundings in which the artefacts were found. Deformed grains and inclusions in the alloys could also affect adversely the corrosion rate. The thickness of the patinas on 1030, 800, 550 and 176 years old artefacts is within the same range, because the rate of the patina growth decreased with time (see Table A–IV): the corrosion rates with the uncertainty bars are illustrated in Figure A–7.

It should be pointed out that both the pre- and post- excavation history of the samples is not well known. Copper and copper alloys have a noteworthy record of durability in soils and in water. New World archaeological bronzes are not different to those from the Old World. The inner layers of patina have the effect of decreasing the corrosion rate.

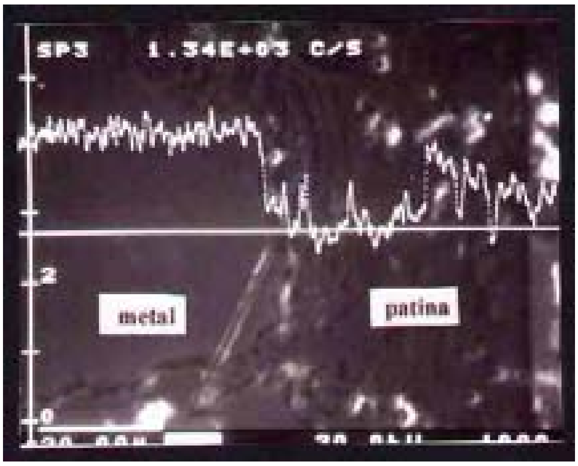

FIG A–3: Chisel, copper profile.

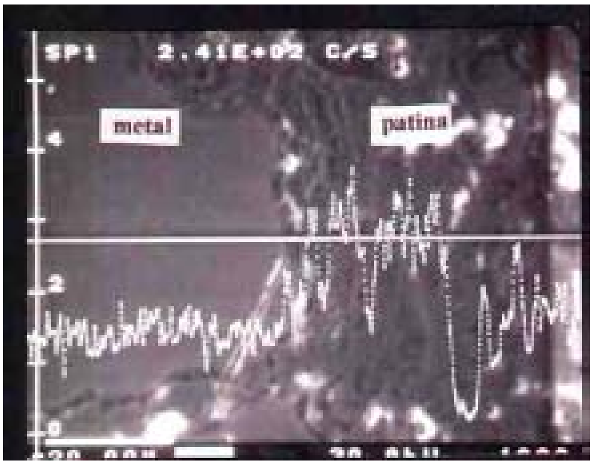

FIG A–4: Chisel, tin profile.

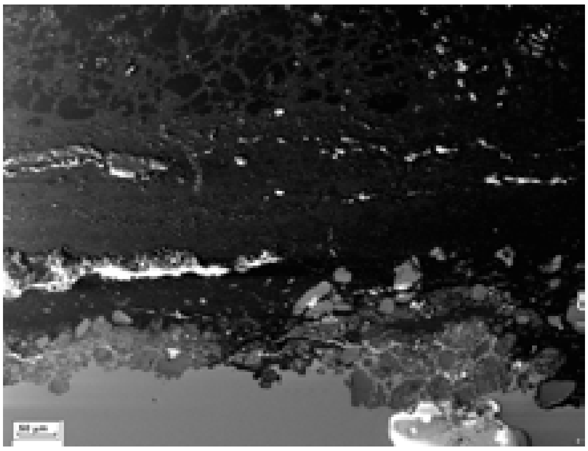

FIG. A–5: SEM image of patina.

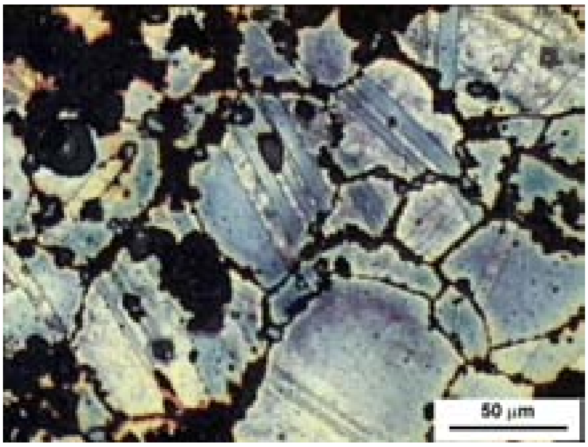

FIG. A–6: Metalography of ancient bronze.

These metals and their alloys could be useful as engineered barriers to contain long lived radioactive waste. The use of these materials will need to take into account not only their durability but also their behaviour in the repository environment. The data presented in this study will be important for a national radioactive waste programme. We think that these results may be used to select materials for container design. The corrosion rates obtained are useful information to define the thickness of container walls.

The other CRP studies carried out on materials from the Ukraine [13] and China [14] have also studied copper alloys archaeological artefacts, with corrosion rates results similar to our own. It must be pointed out that the Ukrainian and Chinese artefacts were mainly manufactured by casting, whilst our samples were hand forged and annealed.

Corrosion rate is the main result that we have measured in this first study on South American archaeological and historical artefacts. In museums, people can observe metal objects more than 7000 years old, still conserving their primitive and recognisable shapes. These include written documents by Assyrian kings on copper and other metals, preserved in stone boxes and placed inside temples and palace foundations or walls, or the copper Dead Sea scrolls kept in ceramic amphorae [15]. It is evident that some ancient cultures planned intentionally for certain objects to endure for long times and this was achieved by selecting a multibarrier systems. This evidence of feasibility of long-term functioning of some materials does not come from laboratory studies but from our history.

TABLE A–IV. AGE, PATINA THICKNESS AND CORROSION RATE OF STUDIED MATERIALS (WITH UNCERTAINTIES)

Sample	**Age** (a)	**Age uncertainty**	**Patina thickness** (µm)	**Thickness uncertainty**	**Corrosion rate** (µm/a)	**Corrosion rate uncertainty**	**Corrosion rate extend. uncertainty**
1	800	40	904	19	1.13	0.01	0.13
2	800	40	64	4	0.08	0.00	0.03
3	800	40	144	25	0.18	0.01	0.07
4	800	40	119	16	0.15	0.01	0.13
5	550	90	445	49	0.81	0.01	0.19
6	550	90	896	161	1.63	0.02	0.05
7	1030	120	137	14	0.13	0.00	0.32
8	1030	120	180	27	0.17	0.01	0.79
9	176	0	61	6	0.34	0.02	0.05
10	176	0	113	14	0.64	0.02	0.07

Note: The extended uncertainty indicate approx. 95 % level of confidence.

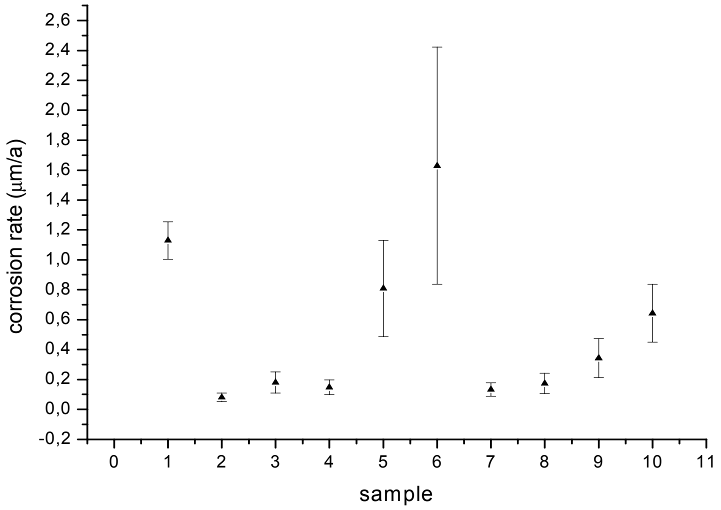

FIG. A–7: Sample corrosion rates, with uncertainties.

REFERENCES

[1] ROBBIOLA, L., BLENGINO, J.M., FIAUD, C., Morphology and Mechanisms of Formation of Natural Patinas on Archaeological Cu-Sn Alloys, Corrosion Science, Vol. 40, 12, 2083 (1998).

[2] UHLIG, H.H., Corrosion and Corrosion Control, 2 nd ed., John Wiley, 165 (1971).

[3] HALLBERG, R.O., ÖSTLUND, P., WADSTEN, T., A 17th Century Bronze Cannon as Analogue for Radioactive Waste Disposal, Natural analogues in radioactive waste disposal, B. Côme and N.A. Chapman (Eds.), CEC report 11037 EN, Graham and Trotman, 135 (1987).

[4] KING, F., A Copper Container Corrosion Model for the In-room Emplacement of Used Candu Fuel, Report AECL-11552 (1996).

[5] BRESLE, A., SAERS, J., ARRHENIUS, B., Studies in Pitting Corrosion on Archaeological Bronzes, Copper, SKB Technical Report TR 83-05, Stockholm, Sweden (1983).

[6] JOHSON, A.B., FRANCIS, B., Durability of Metals from Archaeological Objects, Metal Meteorites and Native Metals", Report PNL-3198 (1980).

[7] AMBROSETTI, J.B., Exploraciones Arqueológicas en la Ciudad Prehistórica de "La Paya" (Valle Calchaquí, provincia de Salta), Publicación de la Sección Antropología 3, Facultad de Filosofía y Letras, Universidad de Buenos Aires, segunda parte, 409 (1908) (In Spanish).

[8] GONZÁLEZ, A.R., DÍAZ, P.P., Notas Arqueológicas sobre la Casa Morada, La Paya, Estudios de Arqueología *5*, 13 (1992) (In Spanish).

[9] TARRAGÓ, M., Areas de Actividad y Formación del Sitio de Tilcara, Cuadernos 3, Facultad de Humanidades y Cs. Sociales, Universidad Nacional de Jujuy, 64 (1987) (In Spanish).

[10] TARRAGÓ, M., GONZÁLEZ, A.R., La Producción Metalúrgica Prehispánica en el Asentamiento de Tilcara. Estudios Preliminares sobre Nuevas Evidencias, Los Desarrollos Regionales y sus Territorios. Arqueología del NOA, Universidad Nacional de Jujuy, 177 (1988) (In Spanish).

[11] VENTURA, B.N., Metalurgia: Un Aspecto poco Conocido en la Arqueología de las Selvas Occidentales, PREP, N° 2 (1985) (In Spanish).

[12] VENTURA, B.N, Síntesis de las Investigaciones Arqueológicas en el Sector Norte de las Selvas Occidentales, Arqueología 1, ICA, Facultad de Filosofía y Letras, UBA, 51 (1991) (In Spanish).

[13] DEMCHENKO, L., MANICHEV, V., SPASOVA, L., ZLOBENKO, B., Research of Stability Materials (Metal, Glass, Ceramics) at Interaction with Containing Breeds (Loess Clay Loam) and Products Metabolism on an Example Archaeological of Monuments Norther Prichernomor'a of Ukraine, IAEA Contract No. 10748/R1, Vienna (2002)

[14] CHEN Z., LIU Y., FAN G., WEN Z., SUN S., LI Y., ZHANG Z., A Study on the Corrosion of Unearthed Bronze Relics, IAEA Contract No. 10744/R2, Vienna (2002).

[15] CURTIS WRIGHT, H., Ancient Burials of Metallic Foundation Documents in Stone Boxes", Occasional Papers, University of Illinois, 157, 1 (1982).

ANNEX B
CHINA

A STUDY ON THE CORROSION OF UNEARTHED BRONZE RELICS

Z. Chen[1], Y. Liu[1], G. Fan[1], Z.Wen[1], S. Sun[2], Y. Li[2], Z. Zhang[3]
[1] Beijing Research Institute of Uranium Geology, Beijing, China
[2] University of Science and Technology, Beijing, China
[3] East China Institute of Technology, China

Abstract

This paper presents compositional analyses and structure observations of bronze relict samples and environmental conditions of the sites where the samples were collected. These bronze samples were taken from the dry region of northern China and the humid region of southern China. Their ages were 1800, 3000 and 3300 years. Research results revealed that the bronze relics had been continuously corroded with time. The corrosion layer consisted of at least two sub-layers, such as oxide and carbonate. There was a mechanical corrosion sub-layer found in few samples (a loose sub-layer). A SnO_2 sub-layer also occurred in a few samples. The thickness of bronze corrosion layers varied with the different climate environments in which the samples were taken. Their thickness was 50–260 μm and 320–800 μm in the dry and humid climate regions, respectively. With respect to natural corrosion resistance, bronze is recommendable as a material for HLW repository system canisters.

1. INTRODUCTION

Research history on the corrosion of bronze is extensive. As early as the 1930s, Collins carried out a corrosion study on early Chinese bronze [1]. But the research on the relevance of copper corrosion to HLW disposal containers was carried out later. Tylecote considered that copper or copper alloy were by far the most suitable material, having shown the greatest resistance to corrosion of all the materials examined [2]. Johnson and Francis revealed a range of copper corrosion rates of 0.025 to 1.27 μm/year, which, due to the harsh environmental conditions, may be considered an upper limit to that expected in a repository [2]. A study of pitting corrosion on archaeological bronze by Bresle [3] is relevant to HLW disposal system in some environments. Swedish scientists made many studies on copper corrosion [4–7].

The Coordinated Research Project on Anthropogenic Analogues for Geological Disposal of High Level and Long Lived Radioactive Waste proposed by the IAEA has been significant for material selection and the design of canisters for a HLW repository system. Assessment of the applicability of metals such as pure copper, carbon steel and stainless steel as candidate materials for canisters for high level radioactive waste has been conducted in some countries [8–10].

China is rich in unearthed bronze relics dating back more than 3000 years. Bronze relics from the west Zhou Dynasty and Shang Dynasty of China, dating from 3000–3300 years, were the research object for the current study on corrosion of unearthed copper relics in different environmental conditions. In order to compare different natural conditions, samples from the Han Dynasty, dated from 1800 years, were also tested within this study.

The objectives of this study were:

- To observe corrosion products of unearthed bronze relics;
- To measure the corrosion thickness of unearthed bronze relics from different environment conditions;
- To analyse the composition of the matrix and corrosion layer of unearthed bronze relics;

- To understand the relationship between the corrosion process and environmental conditions;
- To establish a geochemical model of bronze corrosion in China.

The following work was completed in this study of 15 bronze samples collected from different environmental conditions which represent both dry and humid climate:

- Field investigation of the sites where samples are taken;
- Analyses of the composition of soil and water in the sites where samples were buried;
- Observation of the matrix and corrosion layers of unearthed bronze relics;
- Analyses of the composition of the matrix and corrosion layers of unearthed bronze relics;
- Measurement of the thickness of corrosion layers of unearthed bronze relics;
- Interpretation of the relationship between the corrosion process and environmental condition;
- Establishment of a model of the corrosion process of unearthed bronze relics.

Research results revealed that the bronze relics were continuously corroded with time. The corrosion layer of bronze relics consisted of at least two sub-layers, the oxide and carbonate ones. Sometimes, there could be a mechanical corrosion sub-layer found. A SnO_2 oxide sub-layer also occurred in a few samples. The corrosion products were cuprite, malachite, azurite, stannolite and cerussite. Native copper was identified in a sample. The thickness of bronze corrosion layers varied with the different climate environments to which the samples were exposed, and it was 50–260 μm and 320–800 μm in the dry and humid climate regions, respectively.

2. LOCATION OF THE STUDY

The 15 samples studied were collected from six sites in Northern and Southern China (see Figure B–1). Some information on the sites is presented in Table B–I. The climate conditions in the two regions are characterized in Table B–II.

All of the samples were taken from museum depositories. As ancient cultural relics cannot be damaged, the samples studied could only be fragments, not suitable for restoration into an integral object. As a result, we have not been able to specify the origin of some fragments. The samples were not cleaned and their surfaces were not also been modified prior measurements. In some cases, there was still soil on the surfaces of samples.

TABLE B–I. INFORMATION ON THE SITES

Site	**Province**	**Sample age** (y)	**Found in**	**Soil**
Wuhan	Hubei	3300	Tomb	Red soil
Xingan	Jiangxi	3100	Tomb	Sand
Baoji	Shaanxi	3000	Tomb	Yellow soil
Liulihe	Beijing	3000	Tomb	Yellow soil
Yongning	Guangxi	1800	Cavity	Lateritic red earth
Yizhou	Guangxi	1800	Cavity	Limestone red soil

TABLE B–II. CLIMATE CONDITIONS IN THE STUDY SITES

Climate Factor		Wuhan	Xingan	Baoji	Liulihe	Yizhou
Climate Zone		Sub-tropic zone with humidity	Sub-tropic zone with humidity	Temperate zone with semi-humidity	Temperate zone with semi-humidity	Southern sub-tropic zone with humidity
Temperature (°C)	Ave.	16.3	17.6	12	12	20
	Max.	41.3	40.4	41.6	42	39.9
	Min.	-18.1	-8.9	-16.7	-27	-2.9
Rainfall (mm)	Ave.	1222	1594	700	600	1400
	Max.	2000	1868	1000	1245	1630
	Min.	800	1245	400	275	904
Evaporation (mm)		1400	1426	1340	1813	1445

3. MATERIAL STUDIED

The description of some sample fragments is provided in Table B–III.

3.1. Preparation of samples for analysis

A small piece of sample was cut off from a fragment of a bronze relic and embedded vertically into a round block of polyester along the direction of its long axis. The whole round block with sample was ground and polished in order to obtain an extra smooth surface for microscopic observation. The surface of the polished section was coated with carbon for EPMA measurement.

Water and soil samples for analysis were collected near to the sites where bronze relics were discovered. As some relics were not excavated within this study and were collected from museums, information on geochemical characteristics of their host environment could not be obtained directly.

TABLE B–III. DESCRIPTION OF SOME SAMPLE FRAGMENTS

Sample	Size (cm)	State of preservation	Age
1827-1	NA	NA	3300
1827-2	3.5 x 1	Good	3300
1827-3	2.5 x 2	Good	3300
1827-4	4 x 1.5	NA	3300
1832-1	2 x 2	Very good	3300
1832-2	NA	Good	3300
B2	6 x 2	Good	3000
B3	8 x 5	Good	3000
B10	10.5 x 2	Good	3000
B11	3 x 2.4	Good	3000
L1	3.4 x 1.5	Good	3000
L2	10 x 2.2	Fair	3000
XG	2.5 x 1.8	Good	3100
Y1	15 x 5	Good	1800
Y2	4 x 1.5	Good	1800

FIG B-1. Sites from which the samples originate.

3.2 Analytical methods and results

A Leica DM RX-HC microscope was used in the microscopic observation for polished section of bronze relics. Using a JXA-8600 electron microprobe and a Link eXL energy dispersive spectrometer under the same experimental conditions, EPMA X ray line scan analyses were made on 15 samples. Pure Cu and Pb metals (JEOL, Japan) were used as analytical standards for Cu and Pb analysis, respectively. SnO_2 was used as an analytical standard for Sn analysis (made by C.M. Taylor Company, USA).

A PW-1700 X ray diffractometer was used for identification of corrosion products. Chemical compositions of soil and water were obtained by X ray fluorescence spectrometry and ICP-MS.

In order to investigate the local environmental conditions of the sites of sample origin, water and soil samples were analysed. The results are listed in Tables B-IV and B-V.

Bronzes are alloys of copper with tin. Most ancient alloys have less than 17% Sn [11]. Chinese bronzes usually contain Cu, Sn and Pb [12]. Microprobe analyses of the studied bronze samples have proved that bronzes dating from 1,800~3,300 years ago in China consisted of Cu, Sn and Pb, and contained less than 17% Sn. Electron microprobe analyses of the bronzes studied are listed in Table B–VI. EPMA results for sample B3 are shown in Figure B–2.

TABLE B–IV. CHEMICAL ANALYSES OF SOIL SAMPLES FROM THE DIFFERENT SITES (WT%)

Sample	SiO_2	Fe_2O_3	Al_2O_3	TiO_2	MnO	CaO	P_2O_5	MgO	K_2O	Na_2O	FeO	Loss	pH
Liu1	66.04	4.23	12.1	0.58	0.083	3.32	0.920	1.87	2.35	1.26	1.12	7.75	7.33
Liu2	61.01	4.40	11.9	0.59	0.111	6.88	0.352	2.47	2.37	1.82	1.13	8.84	7.13
Bao1	62.74	6.10	14.6	0.71	0.147	0.10	0.233	2.53	2.88	1.83	1.08	6.82	7.57
Bao2	64.33	5.75	13.8	0.71	0.148	2.07	0.271	2.22	3.01	1.91	1.03	6.07	7.46
Bao3	61.45	5.67	13.8	0.70	0.115	3.52	0.151	2.28	1.72	1.37	1.17	8.76	7.70
Xingan	79.68	1.42	9.05	0.19	0.042	0.44	0.031	0.47	4.92	0.97	0.18	1.64	5.98
Wuhan	67.07	2.39	16.9	0.89	0.017	0.47	0.043	0.84	2.25	0.76	0.52	0.52	5.99
Yizhou	64.73	2.85	11.4	0.38	0.202	1.80	0.128	1.68	2.38	2.71	0.72	11.3	NA

TABLE B–V. CHEMICAL ANALYSES OF WATER FROM THE SITES

Sample	K^+	Na^+	Ca^{2+}	Mg^{2+}	SO_4^{2-}	Cl^-	CO_3^{2-}	HCO_3^-	pH	TDS	Source
Xingan 1	13.5	1.63	3.37	0.64	<0.01	6.31	NA	62.9	5.70	88.33	Natural pool
Xingan 2	2.92	5.06	17.0	5.68	4.07	7.78	NA	56.1	5.63	98.56	Drinking well
Wuhan	3.10	27.2	93.7	20.6	134.6	46.2	7.26	98.01	7.02	430.7	Water in tomb
Yizhou	1.25	1.63	41.9	7.85	43.26	1.08	NA	115.4	7.20	213.0	Natural pool

TABLE B–VI. ELECTRON MICROPROBE ANALYSES OF BRONZE SAMPLES (wt%)

Sample	Measured area	Cu	Sn	Pb
1827-1	Alloy	74.2	9.54	2.40
	Inner layer	26.5	15.6	7.73
	Outer layer	10.1	21.8	10.9
1827-2	Alloy	74.2	8.12	6.18
	Inner layer	53.3	10.6	7.72
	Outer layer	14.9	16.0	15.3
1827-3	Alloy	64.6	11.3	3.05
	Inner layer	26.6	19.7	9.17
	Outer layer	17.7	18.3	10.9
1827-4	Alloy	82.0	10.4	3.97
	Inner layer	27.5	20.5	9.13
	Outer layer	14.7	27.5	9.82
1832-1	Alloy	79.1	11.9	3.85
	Inner layer	19.9	28.0	10.5
	Outer layer	11.1	32.8	9.80
1832-2	Alloy	75.2	12.2	3.31
	Inner layer	17.0	30.0	10.3
	Outer layer	19.0	31.2	8.80
B2	Alloy	86.7	10.8	0.94
	Inner layer	53.5	20.7	2.34
	Outer layer	NA	NA	NA
B3	Alloy	80.9	12.6	1.48
	Inner layer	52.6	17.7	3.29
	Outer layer	45.3	0.22	1.83
B10	Alloy	86.5	8.89	0.65
	Inner layer	76.0	12.5	0.61
	Outer layer	46.2	9.16	1.60
B11	Alloy	66.0	22.7	2.80
	Inner layer	42.8	29.6	2.78
	Outer layer	10.4	44.5	5.07
L1	Alloy	94.0	5.61	0.49
	Inner layer	49.5	17.8	2.72
	Outer layer	36.4	13.6	2.80
L2	Alloy	84.8	12.6	1.41
	Inner layer	21.0	30.4	8.52
	Outer layer	23.8	0.82	4.71
XG	Alloy	80.6	14.8	0.19
	Inner layer	30.8	28.9	1.26
	Outer layer	12.8	36.9	1.56
Y1	Alloy	78.5	11.9	2.32
	Inner layer	47.7	14.0	7.26
	Outer layer	18.7	27.5	10.5
Y2	Alloy	76.8	12.2	2.76
	Inner layer	25.8	21.5	6.77
	Outer layer	18.3	31.0	7.47

Note: Data in this table are average values received at 3 scanned areas.

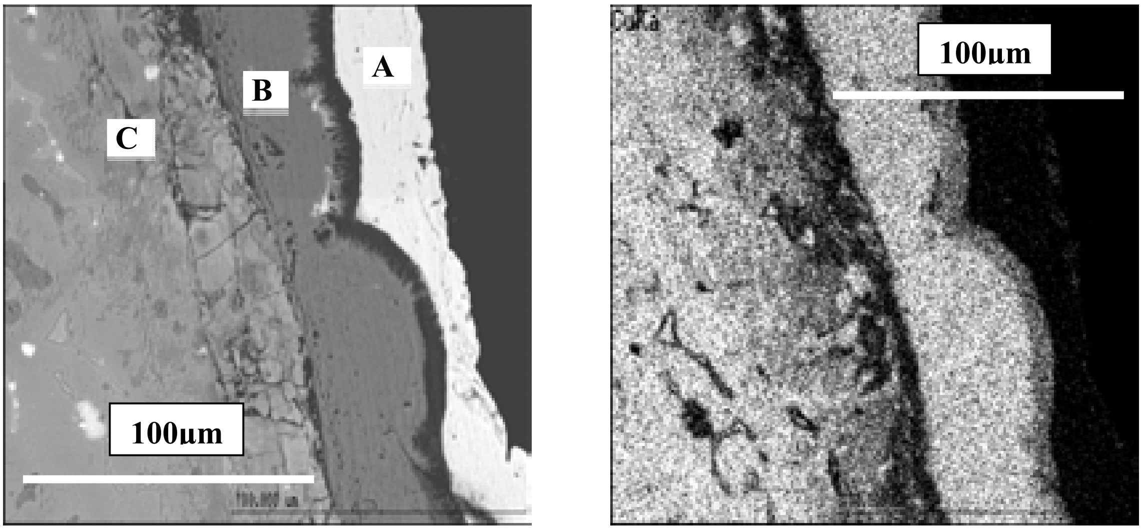

Background electron image of bronze samples (A–carbonate sublayer, B–oxide sublayer, C–bronze matrix)

X ray image of Cu

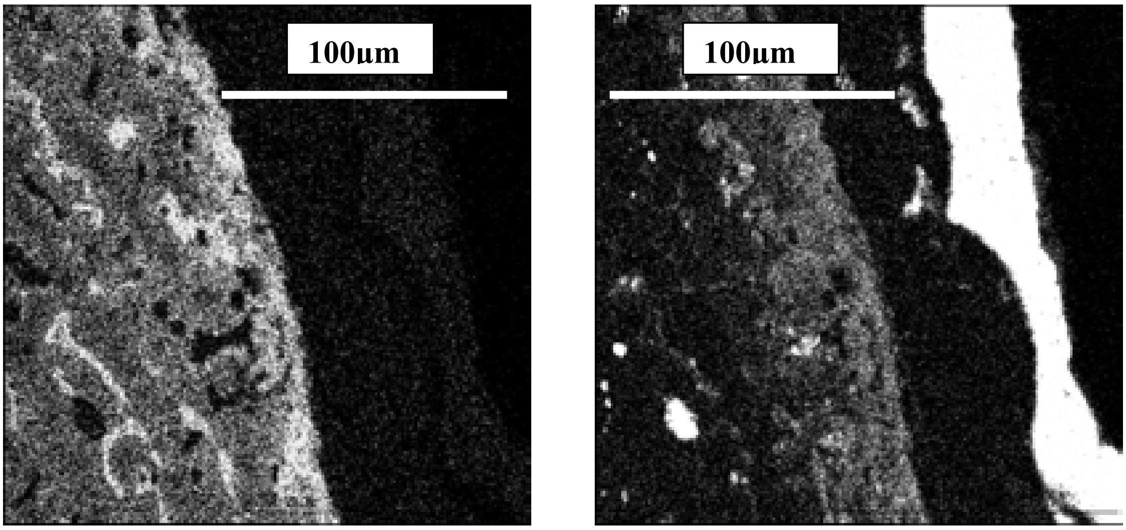

X ray image of Sn

X ray image of Pb

FIG. B–2. Electron microprobe analyses of bronze sample B3.

4. DISCUSSION

4.1. Key findings: Corrosion layer

Corrosion products of copper, such as cuprite, malachite, azurite, cerussite and stannolite, have been identified on the surface of both bronze relics and native copper in deposit [13–15]. Petrographic and stereomicroscopic observation and X ray diffraction measurement of the bronze relics have revealed that the minerals mentioned above occur in corrosion layers.

The layering of corrosion was very obvious under the petrographic microscope. Based on the colour of the corrosion layers of the unearthed bronzes, at least two sub-layers could be identified in most of the samples studied: i.e. red copper oxide sub-layer and green carbonate sub-layer (Figure B–3, B–4).

Some values of the thickness of corrosion layers are listed in Table B–VII. The data in Table B-V indicate that the thickness of the red sub-layers in all the samples is around 100 µm and less than that of the green sub-layers. The thickness of corrosion layers in samples from the dry climate region is around 50~260 µm and less than that from the humid climate region. The corrosion rate is 0.02–0.09 µm/a and 0.10–0.42 µm/a for the dry climate region and humid climate region, respectively.

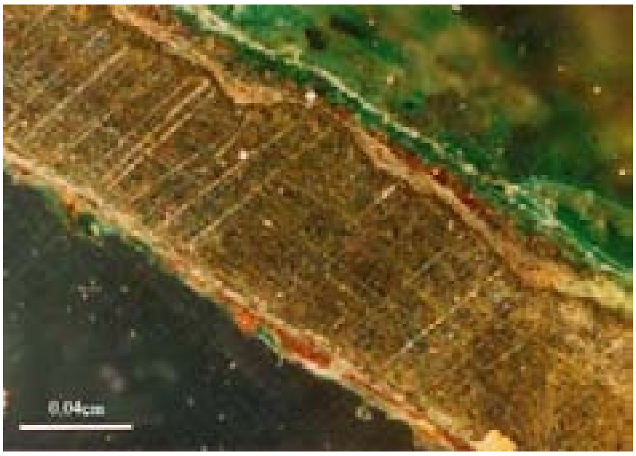

FIG. B–3. Structure of corrosion layer on polished layer for sample 1832-1 under petrographic microscope (The loose sub-layer close to bronzes matrix is in yellow; the oxide sub-layer is in red; the carbonate sub-layer is in green; the bronze matrix is as a long strip in the centre of the picture).

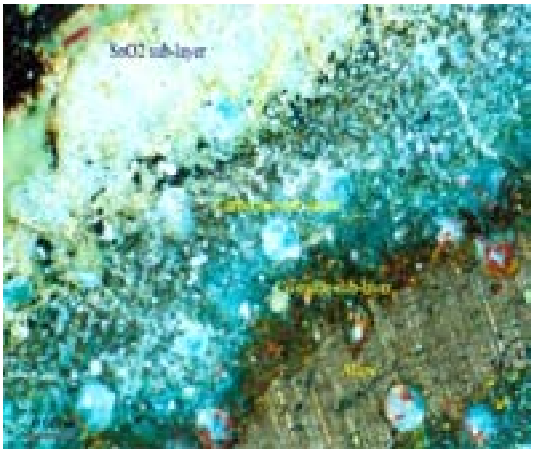

FIG. B–4. Structure of corrosion section for B3 sample under petrographic microscope.

4.2. Key findings: Cu, Sn, Pb migration

In terms of geochemical behaviour of the elements, Cu is the most active among the three major bronze elements (Cu, Sn, Pb). The EPMA X ray line scan analyses (Figure B-5) have demonstrated that Cu was leached out from the bronze matrix: the Cu content in the bronze matrix was generally 75–80%; while in the Cu corrosion sub-layer and outer corrosion layer dropped to around 50% and 10~20%, respectively.

The trend for Sn was a concentration increase from the inner part to the outer layer in the bronze. There was no significant change of Pb content in the scanned profiles.

4.3. Effect of environmental conditions on the corrosion process

Our research results have revealed that natural environmental conditions greatly affected the corrosion degradation of bronze. Collins considered that “mineralization of bronze appears to have been more high developed in China than in any other country in the world” [1]. This study dealt only with samples from the loess region in central China. However, some research results in this project are coincident with the afore mentioned statement.

TABLE B–VII. THICKNESS OF CORROSION LAYERS OF UNEARTHED BRONZE (ALL VALUES ARE IN µm)

Sample No.	Red sub-layer	Green sub-layer	Yellow sub-layer
1827-4	150	160	350
1827-3	300	200	100
Y1	300	400	NA
Y2	300	450	NA
L1	40	60	NA
XG	200	250	NA
1832-1	100	400	300
1832-2	120	200	0
1827-2	100	300	200
B3	200	60	NA
L2	20	140	NA
B2	50	100	NA
B11	20	30	NA

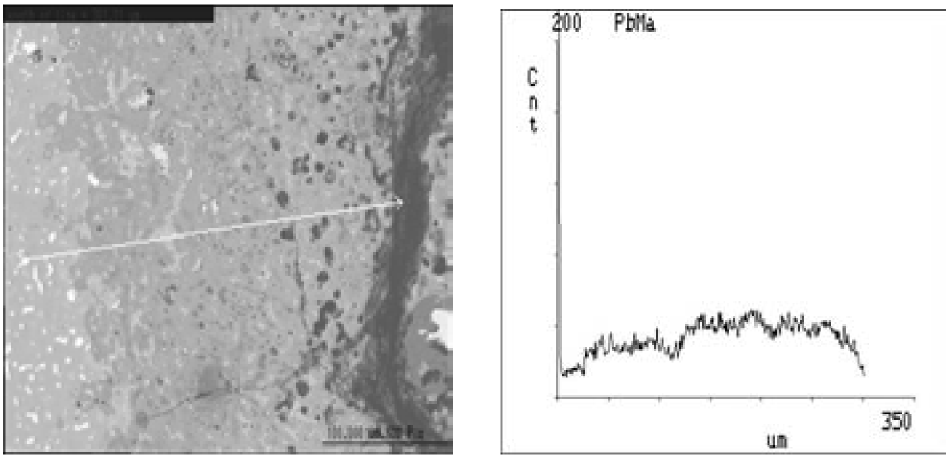

Backscattered electron image

X ray scan line of Pb

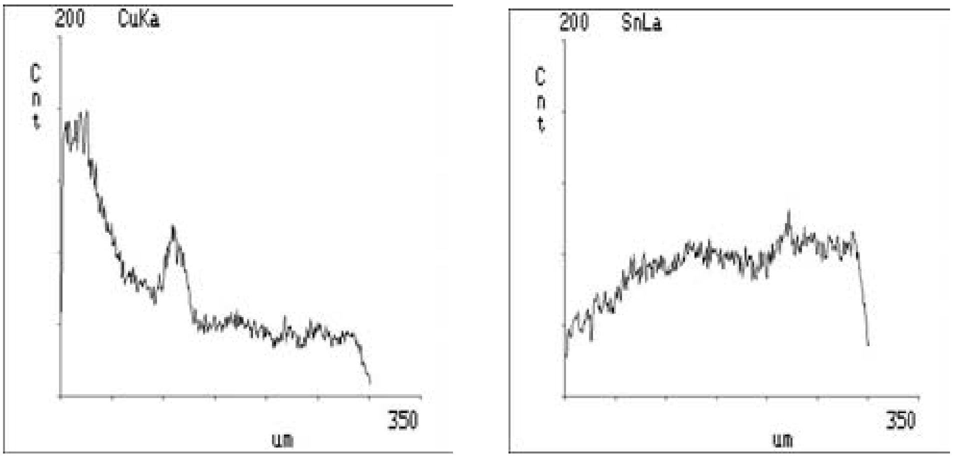

X ray scan line of Cu

X ray scan line of Sn

FIG. B–5. EPMA X ray line scan analyses for sample 1832-1.

Corrosion products of samples from the Baoji and Liulihe sites, situated in the loess region in central China, such as cuprite, malachite, azurite cerussite, were massive and crystalline, like natural minerals. But the occurrence of minerals from the humid region of southern China differed from that in the region mentioned above, and was in cryptocrystalline form, or created amorphous or discontinuous aggregates. The thickness of the corrosion layers from this region was lower than from the humid region.

5. ANALOGUE

According to the disposal concept in Sweden, spent fuel should be encapsulated in cylindrical cast iron canisters that have an outer 50 mm thick shield made of copper and emplaced in crystalline rock at a depth of about 500 m [4].

Based on our research results, the maximum depth of bronze corrosion is 270 μm/1000 years, in the dry climate environmental condition. Thus, after 100 000 years, the total depth of general corrosion may be only 27 mm (compared to the canister thickness of 50 mm). When bronze material is stored in reducing environment and dry climate conditions, the corrosion rate is even reduced.

The project *"Siting and site characterization study for China's high level radioactive waste repository*" has been initiated in the Gobi Desert, Beishan area, Gansu Province, NW China. The precipitation in the Gobi Desert is less than 100 mm/a, therefore, the climatic conditions in the Gobi Desert are prospective for emplacement of bronze canisters.

Speaking from the viewpoint of material corrosion resistance, bronze is thus available as a material for canisters for the Chinese geological repository system.

5.1. Uncertainties

Our research results were obtained under oxidizing condition. However, the repository environment will be in reducing environment. Bronze materials have to be resistant to the impacts of radiation, heating and mechanical attack, and this was not addressed in this study.

A patination film protects the metal from corrosion [1]. There are uncertainties regarding its anticorrosion effectiveness in relation to patina thickness, namely if the growth of patina is stopped or slowed down.

5.2. Comparisons

Scientists have had different research viewpoints on corrosion behaviour of bronze. Zlobenko demonstrated that different degrees of corrosion depended on the material composition resulting from casting [16] while Palacios assumed that corrosion was hardly dependent on the kind of soil and the environment in which the artefacts were found, and, also, that deformation and grain inclusions of the alloy adversely affected the corrosion rate [17]. Pitting corrosion was not observed in neither Palacios's nor this study.

Our study has shown that the corrosion process of bronze was affected by environmental conditions such as climate and the chemical composition of soil and ground water.

5.3. Future studies

The potential site of the HLW repository in China is in Gansu province. There are also many archaeological bronze items found in this region. The regional environmental conditions are similar to that in the potential site. Samples for future studies on the corrosion of bronze should thus be collected from Gansu province so that the study results might be directly used for material selection and design of HLW canister.

Research on radiation and heat stress of bronze materials should be also conducted in the future.

ACKNOWLEDGEMENTS

The authors are grateful to Dr. M. Raynal and M. Knapp for technical guidance and Liu Hongbin, the section chief of Baoji Municipal Cultural Relic Administration, Hu Zhiaheng, director of Baoji Bronze Museum, Zhang Ensian, director of Zhouyuan Bronze Museum, Zhao Fusheng, vice director of Beijing Cultural Relic Research Institute, Liang Fulin, head of Management House for Culture Relics in Hechi City, Li Churong, head of management house for Culture Relics in Yizhou County for providing some samples, as well as to Prof. Sun Shuyan and Li Yanxing from the University of Science and Technology, Beijing, for their technical support. The International Atomic Energy Agency and the CNNC supported the research financially.

REFERENCES

[1] COLLINS, W. F., The corrosion of early Chinese bronzes. Journal of the Institute of Metals, Vol.45 (1931).

[2] MILLER W., Natural Analogue Studies in the Geological Disposal of Radioactive Waste, NAGRA Technical Report 93–03 (1993).

[3] BRESLE, A., et al., Studies in Pitting Corrosion on Archaeological Bronze, SKB-83-05 (1983).

[4] KING F., et al., Copper Corrosion under Expected Conditions in a Deep Geologic Repository, SKB-TR-01-23 (2001).

[5] TAXEN, C., Pitting Corrosion of Copper and Equilibrium - Mass Transport Study, SKB-TR-02-22 (2001).

[6] TAXEN, C., Pitting Corrosion of Copper and Equilibrium – Further Model Studies, SKB-TR-02-23 (2001).

[7] KING, F., Corrosion of Copper in Alkaline Chloride Environments, SKB-TR-02-25 (2001).

[8] WERME, L., et al., Twenty-five Years on Progress in the Understanding of the Long-term Corrosion Behaviour of Copper Canisters, SKB-TR-90 (1999).

[9] MATTSON, E., Recent SKB Studies of Copper Canister Corrosion, SKI-R-95-6 (1995).

[10] Research and Development on Geological Disposal of High Level Radioactive Waste, PNC TN1410 93-059 (1993).

[11] SCOTT, D.A., Metallography and Microstructure of Ancient and Historic Metals, The Getty Conservation Institute and J.Paul Getty Museum (1991).

[12] CHASE, W.T., Chinese Bronze and Microstructure, Proceedings of the Forum of the 4th International Conference on the Beginning of the Use of Metals and Alloys, Shimane, Japan (1996).

[13] GERWIN, W., et al., Effect of Soil Parameters on Corrosion of Archaeological Metal Findings, Geoderma 96 (2000).

[14] MILODOWSKI, A.E., et al., Alteration of Uraniferous and Native Copper Concretions in the Permian Mudrocks of South Devon, United Kingdom, SKB TR-02-09 (2002).

[15] SUN, S., et al., The Study of Corrosion Products of Ancient Copper Drum in Guanxi Autonomous Region and Yunan, Guizhou Province, Press of University of Science and Technology Beijing (1994) (in Chinese).

[16] ZLOBENKO B., Research of Stability Materials at Interaction with Containing Breeds and Products Metabolism on an Example Archaeological Monuments of Northern Prichernomorya of Ukraine, IAEA Second RCM on Anthropogenic Analogues for Geological Disposal of High Level and Long Lived Radioactive Waste, Vienna (2002).

[17] PALACIOS T.A., Studies on the Behaviour of Ancient Man-made Materials as Analogues to Materials Used for the Disposal of High Active and Long Lived Waste, IAEA Second RCM on Anthropogenic Analogues for Geological Disposal of High Level and Long Lived Radioactive Waste, Vienna (2002).

ANNEX C

CZECH REPUBLIC

ANTHROPOGENIC ANALOGUES IN THE CZECH REPUBLIC — STUDIES ON GLASS AND CONCRETE MATERIALS

A. Laciok, P. Rajlich, S. Palagyi
Nuclear Research Institute, Řež, Czech Republic
Cooperation:
Faculty of Natural Sciences, Charles University, Prague, Czech Republic
Nuclear Physics Institute, Czech Academy of Sciences, Řež, Czech Republic

Abstract

Uranium glass corrosion/dissolution and concrete-radioactive water interactions were studied as anthropogenic analogues in the Czech Republic, with minor attention also paid to slags. Uranium glasses deposited in natural environments for approximately 80 years were characterized by chemical analyses, microprobe profiling, gamma spectrometry, ETA and a variety of advanced surface characterization methods (PIXE, RBS, ERDA). Thicker alteration zones (100–500 μm) were identified as being depleted in K and Na (partially also in U) with relative enrichment in SiO_2. The estimated corrosion rate was 1.25–6.25 μm/a. PIXE and RBS measurements indicated approximately 10fold enrichment of U in superficial altered layers (0.5–2.3 μm) in comparison with the glass matrix. Studied concrete samples of different age (80 and 10 years) revealed the trend in phase transformations from less stabile phases (ettringite, portlandite) to more stabile minerals (smectite, zeolite) in hardened cement matrix. Performed leaching tests showed immense pH buffering capacity of concrete that is favourable factor for immobilization of radionuclides in hyperalkaline environment. Low measured concentrations of U and Th indicated low mobility of these elements.

1. INTRODUCTION

Anthropogenic analogues can be valuable source of information about the long-term behaviour of materials that are planned to be used or have been used in the repository structure. Information on processes and their quantification for such materials can be used in performance assessment of both near-surface and deep geological repositories. The value of anthropogenic analogues lies mainly in providing additional and complementary information to the data obtained from well-defined laboratory and field experiments; in rare situations they can also provide data directly utilizable in performance assessment calculations. The use of anthropogenic analogues in explanations for the general public and stakeholders is also beneficial.

In the Czech Republic, mainly uranium glass and cement materials were studied, with minor attention also paid to slags (as potential analogues for crystalline-glass waste forms). The selection of these materials was based on two aspects:

- The disposal strategy of radioactive waste and materials planned to be used in the Czech Republic;
- Availability of potentially suitable materials.

The waste disposal strategy in the Czech Republic is briefly described in order to justify the selection of the materials studied.

1.1. Waste forms

Low stress compactor compresses compressible solid radioactive wastes from NPPs into 200 litre barrels. Uncompressible solid wastes (iron, various items from other materials) are embedded in cement (in 200 litre barrels). Liquid radioactive wastes are solidified by bituminisation. Radioactive waste from non-fuel cycle facilities is centrally treated and conditioned in NRI Rez. Liquid wastes are solidified in cement in 200 litre barrels. Solid wastes are embedded in cement in 200 litre barrels.

1.2. Disposal facilities

Excluding the Hostim subsurface repository, operated in 1950–60s (currently being finally sealed), there are three near-surface repositories in operation:

- The Dukovany surface repository (operated since 1994) situated at the Dukovany NPP site is used for operational radioactive waste from NPPs. The repository is composed of two double-rows of **reinforced concrete vaults** (5.4 × 5.3 × 17.3 m) with a total volume of 55 000 m^3 (may accept approx.180 000 drums).
- The Richard and Bratrstvi subsurface repositories are situated in abandoned limestone and uranium mines, respectively, and used for disposal of institutional radioactive waste. Approximately 6000 m^3 of radioactive waste packages could be disposed of in these repositories.

A deep geological repository is under development. The current concept is based on direct disposal of spent nuclear fuel in steel disposal containers in a granitic host rock formation (six regions were pre-selected). Bentonitic materials would be used as buffer, backfill and sealing materials. Concrete will be used in some structures and plugs.

The reprocessing of spent nuclear fuel from NPPs has not been finally excluded and if applied the glass waste forms will be available for disposal.

1.3. Analogue materials

Natural glasses (see [1] for review) have been studied for years as natural analogues of vitrified highly radioactive wastes from reprocessing of spent nuclear fuel [2–3]. Two general types of glass are in focus: high-silica content (rhyolitic glasses and tektites) and low-silica content glasses [4]. Man-made glasses (generally with high content of silica) have been produced for 3500 year.

The kinetics of glasses dissolution is governed by water diffusion - hydration in glass network - ion exchange and network dissolution. Both parallel and sequential reactions occur in the overall dissolution mechanism [5]. Dissolution models are derived from irreversible thermodynamics and transition state theory and expressed in various forms of the first-order rate law (see [6] for review). Leaching experiments were performed frequently with HLW glasses or doped artificial glasses both in the laboratory (a huge body of literature) and in field experiments. Such experiments can provide information used in performance assessment calculations [7]. Interactions of clay with glass have been studied recently [8–9]. It was proved that uranium in surface hydrated layers converts to uranyl-like coordination at the surface [10].

Motivation of the U glass study: Little is known about the dissolution and degradation of anthropogenic glasses in natural environments — [11} as a rare example. Moreover, the presence of uranium in a glass matrix can allow study on the release of uranium and the role of the surface layer.

Concrete materials are widely used in radioactive waste management (waste matrix, sealing material, plugs, rock supports and reinforced structures, etc.). Therefore, data on its stability, degradation and transformation are needed. Natural analogue studies focused on ancient mortar and concrete [12], medieval materials and modern concrete (Portland type) - dams, tunnels, water tanks [13]. Cement undergoes complex reactions during hardening and aging [14]. It was proven that CSH compounds (calcium-silica-water) as binding elements of the concrete are stable over historical and even geological periods. Leaching tests of historical concretes are well established [15–17], but little attention was focused on measurement of diffusion profiles of trace elements.

Motivation of the concrete material study: The study was focused on the durability of modern concrete (degradation and transformation phase composition), concrete-water interactions and migration of radionuclides from high activity natural water.

2. LOCATION OF STUDY

Locations from which the samples were gained are indicated in the Figure C–1.

Uranium glass products (vases, tumblers, ash trays, gift items, etc.) are included in many museum exhibitions in the Czech Republic. F. Reidel invented colouring of glass by uranium in 1830. Uranium glass was then produced in many factories, mainly in Adolfov and Kristianov (Jizerske hory Mountains), Harrachov (Giant Mountains — Krkonose), glassworks in the Silesian part of Giant Mountains, Jablonec (Gablonz) and in South Bohemia (near Kasperske Hory town). Uranium glass was produced in two colours — yellow and green. The usual content of U is approx. 0.1–2 wt%. It is estimated that throughout the 19th century more than 150 t of uranium oxide were consumed and more than 15 000 t of uranium glass were produced. Uranium was used in the form of “uranium yellow” ($Na_2U_2O_7.xH_2O$); in the 1970s depleted uranium was also tested for this purpose.

Fluorescence in UV spectra (an important detection factor in the field) is typical characteristic of uranium glass — intensive green fluorescence is caused by $(UO_2)^{2+}$; on the other hand $(UO_4)^{2-}$ and $(U_2O_7)^{2-}$ does not cause this effect. Also U^{4+} appearing as a product of reduced melting does not fluoresce.

Based on previous investigations, Klastersky Mlyn near Rejstejn town (Kasperske Hory area) was selected as a suitable site for the collection of samples. Relatively good availability of glass samples (outcrops with possibility to obtain samples) and existence of historical sources about glass production (written material, information from local — museum) were the main reasons.

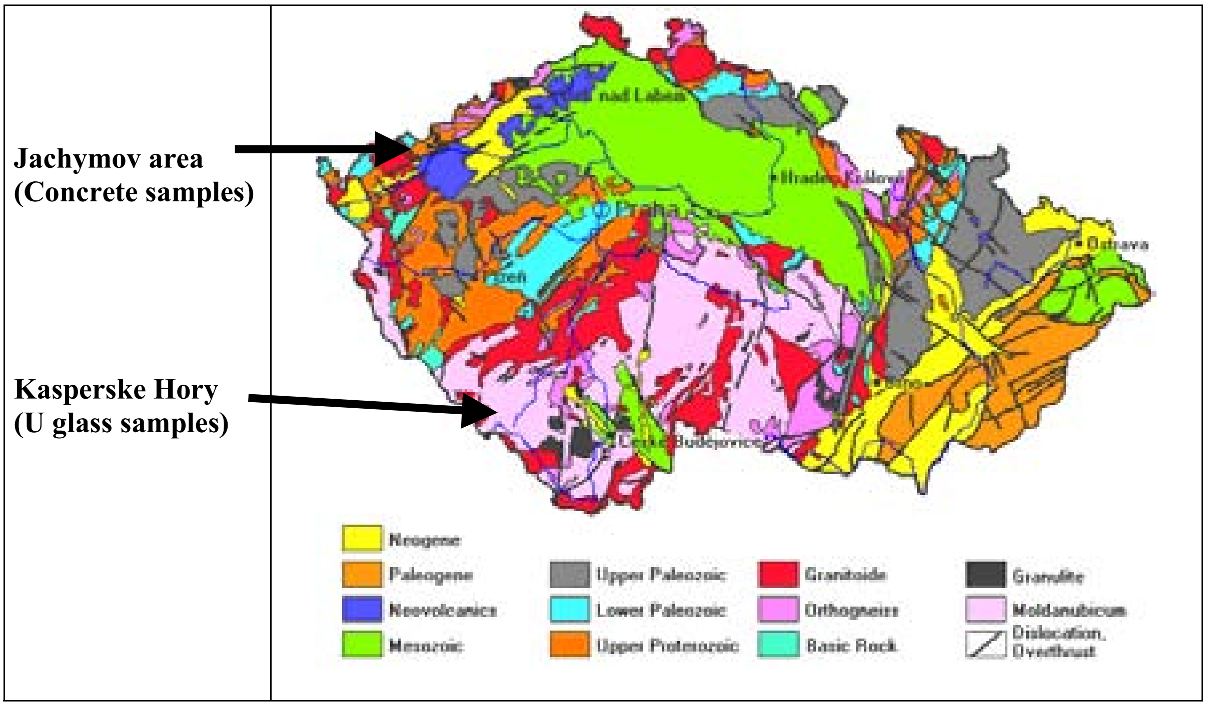

FIG. C–1. Simplified geological map of the Czech Republic with study sites.

Uranium glass was produced there in the period from 1836–1947. The variability of uranium glasses produced was properly documented. The main periods of production are as follows:

— The oldest period - scarce information;

— 1850–1880 — green and turquoise opaque alabaster glass;

— 1880–1910 — various colours — glass imitated semiprecious stones (serpentine, agate, jasper, etc.); marquetry glass;

— 1920–1930 — alabaster glass; Art Nouveau style glass;

— Since 1930 — declining period.

The measured concentration of uranium in the soil profile was in the range of 3.3 to 56.5 ppm. The petrographic composition of the profile and other relevant soil parameters (pH, beta activity, radioactive elements) are shown in Figure C–2.

Concrete material from Svornost mine (Jachymov town) was selected as suitable material. Svornost mine is currently used only for pumping and collection of radioactive water from underlying granite using several boreholes (“springs”) — total inflow from the rock is approximately 370 l/min; activity of water mixed from springs is maximum 12 kBq/l.

Three concrete basins (from which the samples were taken) are used for collection and storing radioactive waters before their distribution to the local spa (established in 1906):

— 12th level (approx. 500 m below the surface) — 100 m^3 basin built in 1924;

— Barbora level (approx. 100 m below the surface) — 2 basins were built here:

- 160 m^3 basin built in 1924 — used until 1995 and again since 1999;
- 300 m^3 basin built in 1995 (a different construction in comparison with older basins).

The great advantage of concrete samples from Svornost mine lies in their nearly permanent interaction with higher radioactivity water of known composition.

3. MATERIAL STUDIED

3.1. Uranium glass

The glass samples were collected in two field campaigns. In total, about 20 kg of glass items were obtained from an old glass landfill that was partially exposed to previous flooding (Figure C–3 to C–6). The horizon with glasses has a thickness of about 40 cm. The collection was focused mainly on green alabaster glass — non-translucent turquoise coloured glass (approximately 80 years old). The horizon with glass is situated about 50 cm below the current surface. Uranium glass samples were cleaned only by water in order not to impair corrosion layers.

3.2. Concrete material

Two oriented samples of concrete were collected by drilling in the floor — from older (SJ sample) and younger concrete basins (NJ sample). The macroscopic appearance of samples was different. The SJ sample was very porous (with high content of clastic component - crashed rock of black colour), but very rigid. The NJ sample was compact, with a finer clastic component, but its rigidity was lower.

Micro-description of SJ sample: The upper and lower parts are not significantly different. The coarse gravel fraction is formed by basaltic rock (foidite, bazaltoide or bazanite) of angular or subangular shape (0.25–15 mm). Gravel is partially altered or fresh. The concrete phase is formed by crypto- to micro-aggregate of carbonate uniformly coloured by Fe oxide. Quartz is only a minor phase.

Micro-description of NJ sample: The upper and lower parts are not significantly different; only minor changes in granularity and pigmentation were identified. The concrete matrix is white-grey to pale pink colour. The clastic (sand and gravel) phase is formed by quartz (90–95%, maximum dimension 10 mm); plagioclase (finely tarnished by Fe oxides) and feldspar (sericitized in some parts) are present only sporadically. The concrete matrix is formed by clay-carbonate crypto- to micro-aggregate uniformly coloured by Fe oxide. Biotite and muscovite occur only sporadically. The part near to the contact with water is characterised by higher proportion of fine grains (dimensions to 0.5 mm) and minutely higher portion of pigment in concrete matrix; authigenic carbonate was also identified.

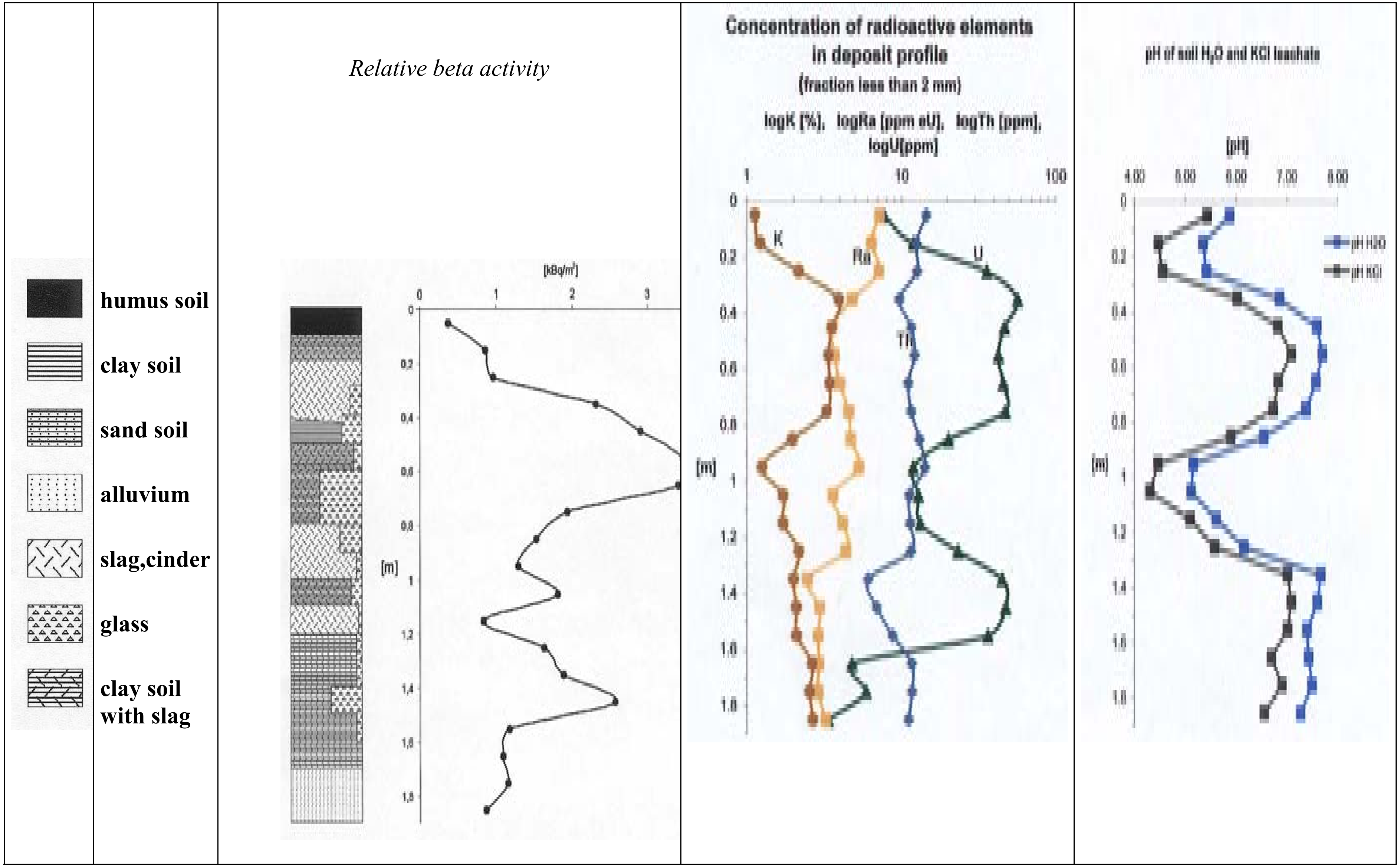

FIG. C–2. Soil characteristics at Klastersky Mlyn site.

FIG. C–3. Glass samples of various colours.

FIG. C–4. Uranium glass attached to furnace liner.

FIG. C–5. Samples of uranium glass.

FIG. C–6. Samples of uranium glass selected for detail characterization.

4. ANALYTICAL METHODS

4.1. Uranium glass

The following analytical methods were employed in testing the glass samples:

— Gamma spectrometry;

— Optical and electron microscopy and electron microprobe (CAMECA SX 100);

— Advanced surface characterisation methods for characterisation of concentration of selected elements in superficial zone or in profile:

- PIXE (Particle Induced X ray Emission) — the effective thickness (over which the concentrations are averaged) was approximately 30 μm;
- RBS (Rutherford Backscattering) — the accessible depths were 0.5 μm (alpha particles) and 2.3 μm (protons);
- ERDA (Elastic Recoil Detection Analysis) — the accessible depth was approximately 0.6 μm.

- — Emanation Thermal Analysis (ETA) — Emanation release rate E (radon release from the sample) is measured during heating of samples from 20–1000°C, formed by the spontaneous alpha decay of Th-228 and Ra-224 incorporated into samples from the surface due to the recoil. The increase in the radon rates (E) indicates an opening of the structure and/or the increase of the surface area of the interfaces, whereas the decrease in E reflects a densification of the structure, closing pores and/or the decrease in the surface area of the interfaces [18].

4.2. Concrete material

The strategy of characterization was focused on changes in chemical and physical composition of concrete in the vertical direction — from the top part (in contact with water collected in the basin) to the lower part of the samples (generally indicated in numbers from 1 to 4) — see Figure C–7 and C–8. The following techniques were used:

- — Optical microscopy (Figure C–9 and C–10);
- — Porosity determination (Hg porosimetry);
- — Basic chemical analyses:
    - Quantitative silicate analysis;
    - Semi-quantitative RTG — mineralogy;
    - Measurement of composition of the selected points by EDS.
- — Radioelements determination:
    - Ra by gamma spectrometry;
    - Radioelements by ICP–MS.
- — Leaching tests (HCl leaching medium, pH = 3).

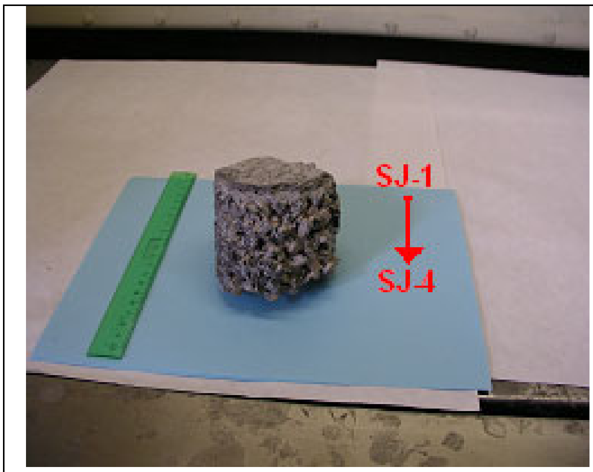

FIG. C–7. SJ sample (top - contact with water).

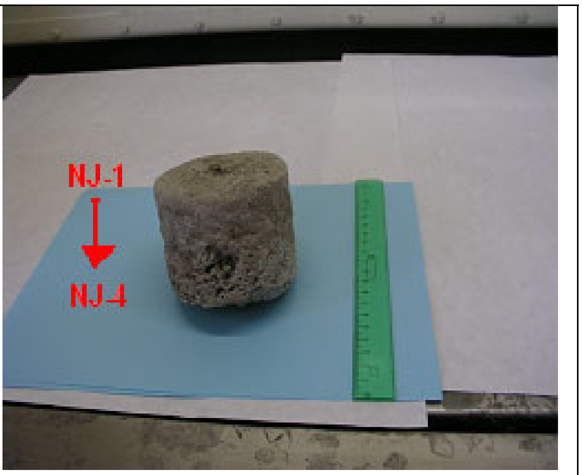

FIG. C–8. NJ sample (top - contact with water).

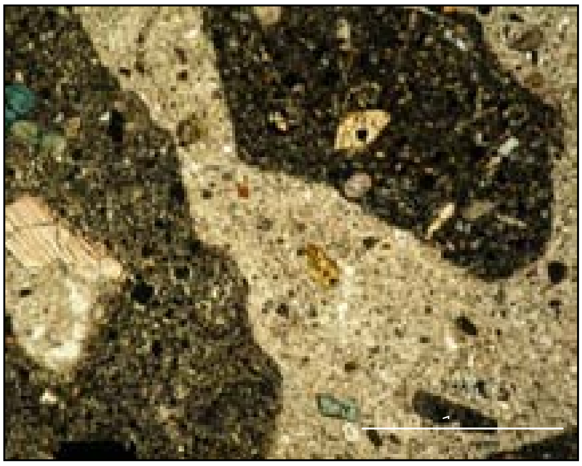

FIG. C–9. Microphotography of SJ sample.

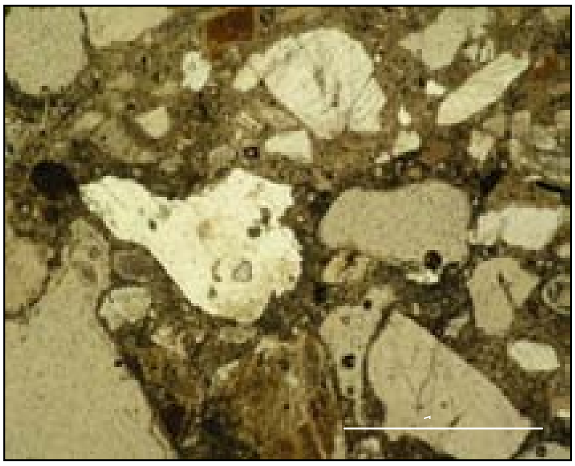

FIG. C–10. Microphotography of NJ sample.

5. RESULTS

5.1. Uranium glass

Glass samples contain typically 0.1–0.4 wt% of uranium. Higher concentrations are not so frequent. The concentrations at the level of several wt% mentioned in the literature were not identified - such items were produced in different glassworks or in different periods.

Optical microscopy revealed the roughness of surfaces (Figures C–11 and C–12) and the relatively high inhomogeneity of glass matrix.

Electron microscopy and microprobe: Backscattered electron images revealed a surface altered layer with lower atomic weight than the matrix - the thickness of the altered layer is in the range of 70–200 µm (gray zones; the unaltered glass matrix is white or greyish). The transition between both phases is sharp, without any intermediate zone (Figs C-13 to C-16).

The uranium glass was identified as an alkaline calcium type. The mean concentration (in the matrix) of SiO_2 is 76 wt%, K_2O 8–17 wt %, Na_2O 1.3–7.5 wt%., CaO 2.4–5.4 wt%. The concentration of P_2O_5 was in the range of 0.3–2 wt%. The glass also contains As_2O_3 at 1.45–5.8 wt% (arsenic has also been found in old recipes for uranium production).

The microprobe profile measurement of some elements (Figure C–17) identified the following trends (matrix → surface layers):

- Marked regular depletion of K_2O from 20 wt% to 2–3 wt%, Na_2O from 1.5 wt% to 0.1-0.2 wt%, UO_2 from 2.2–2.3 wt% to 0.7–0.8 wt%
- Regular increase of SiO2 from 72 wt% to 80 wt% and less regular of CaO in tenths of wt%.
- Variation of P_2O_5, Al_2O and MgO close to or directly into the alteration zone.

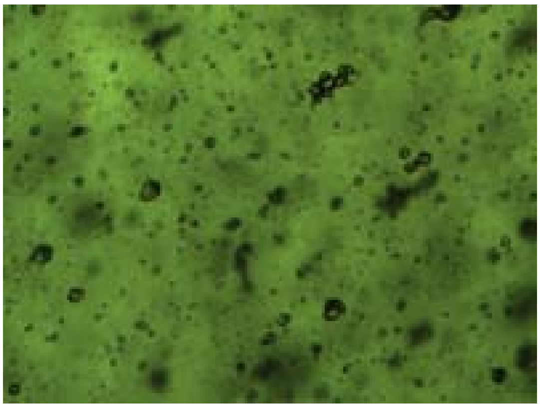

FIG. C–11. Structure of glass (75×5 magnification).

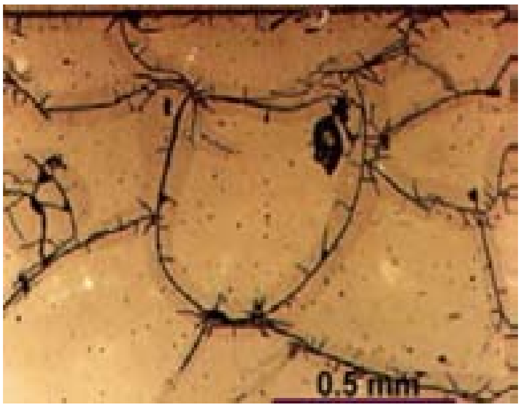

FIG. C–12. Altered glass surface — parallel nicols.

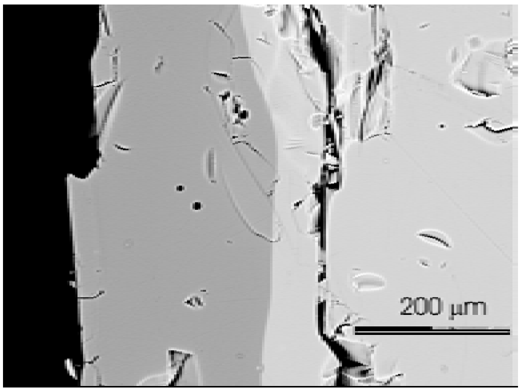

FIG. C–13. Backscattered electrons - structure of altered zone of the glass (profile 1 in the Figure C–17).

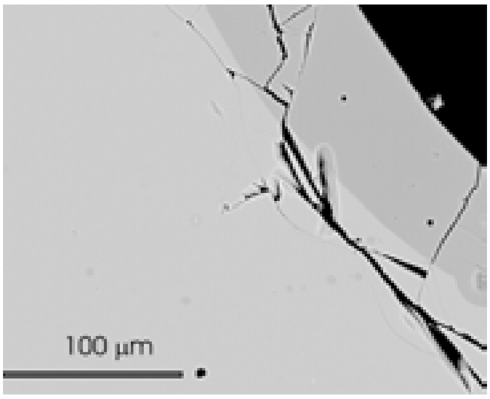

FIG. C–14. Backscattered electrons - structure of altered zone of the glass (profile 2 in the Figure C–17).

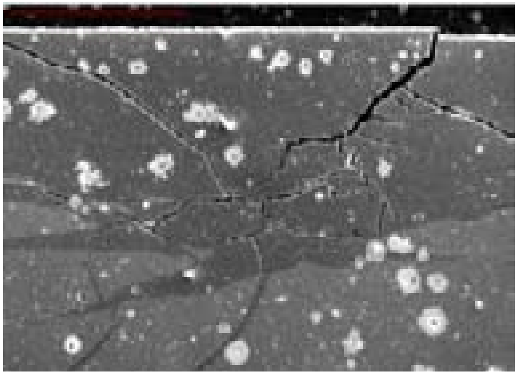

FIG. C–15. View in secondary electrons (bubbles are remarkable).

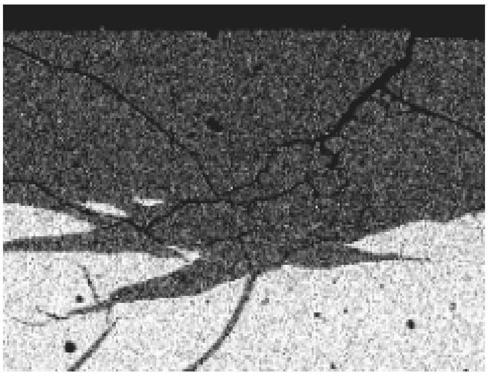

FIG. C–16. Areal distribution of K (higher concentration is whiter).

Advanced surface characterisation methods: Four samples of uranium glass were studied by PIXE and RBS methods (Table C–I and C–II), two samples by the ERDA and altered/unaltered glass surfaces were characterized also by the ETA.

The PIXE method is based on the detection of the characteristic RTG ray initiated in the sample by the beam of accelerated ions.

The RBS method consists in the detection of ions elastically distributed on the atom cores of the investigated sample. Along with the identification of the target ions following their mass it allows for determination of the concentration profile. It is impossible to distinguish the K and Ca signals with the RBS method. The K value in the case of the RBS method gives the sum of the concentration of both elements.

The principle of the ERDA method is the equilibration of the lighter atomic cores by heavier accelerated ions. Both measured samples contained nearly 15 at% of hydrogen, with its slightly higher concentration in the superficial, 50–100 nm thick layer (+ 20%).

Two different surfaces (altered and unaltered matrix) of uranium glass were characterised by emanation thermal analysis (ETA) spectra (x — temperature, y — energy in arbitrary units). Measurement of radon emissions was performed in two different time periods (early after spiking and 5.5 months after spiking) with the aim of characterising different depths of glass (Figure C–18).

TABLE C–I. CONCENTRATION OF SELECTED ELEMENTS DETERMINED BY PIXE. EXTREME VALUES (OUTLIERS) OF K AND Mn WERE OMITTED IN THE AVERAGES.

	K (wt%)	**Ca** (wt%)	**U** (ppm)	**Fe** (ppm)	**Mn** (ppm)	**Cu** (ppm)	**Zn** (ppm)	**Ti** (ppm)	**V** (ppm)	**Rb** (ppm)	**Zr** (ppm)	**Pb** (ppm)
Range	1.8 – 14.9	1.4 – 2.3	3660 – 6260	244 – 653	9 – 110	1180 – 3070	26 – 264	127 – 186	32 – 41	<100 – 445	68 – 92	104 – 365
Average	13.0	1.7	5183	419	11	2098	109	167	35	236	84	233

TABLE C–II. CONCENTRATION OF SELECTED ELEMENTS MEASURED BY THE RBS AND PIXE METHODS

Method	**Depth** (μm)	**K + Ca** (%)	**Ca** (%)	**Si** (%)	**O** (%)	**U** (ppm)	**Cu** (ppm)
PIXE	30	1.9 – 14.9	1.3 – 2.3	NA	NA	3700 – 6300	1200 – 3100
RBS (2.7 MeV He)	0.5	4.5 – 12.1	NA	39.1 – 45.1	43.1 – 50.9	3600 – 9200	2800 – 5900
RBS (2.8 MeV p)	2.3	5.4 – 12.9	NA	NA	NA	3800 – 8600	4900 – 23600

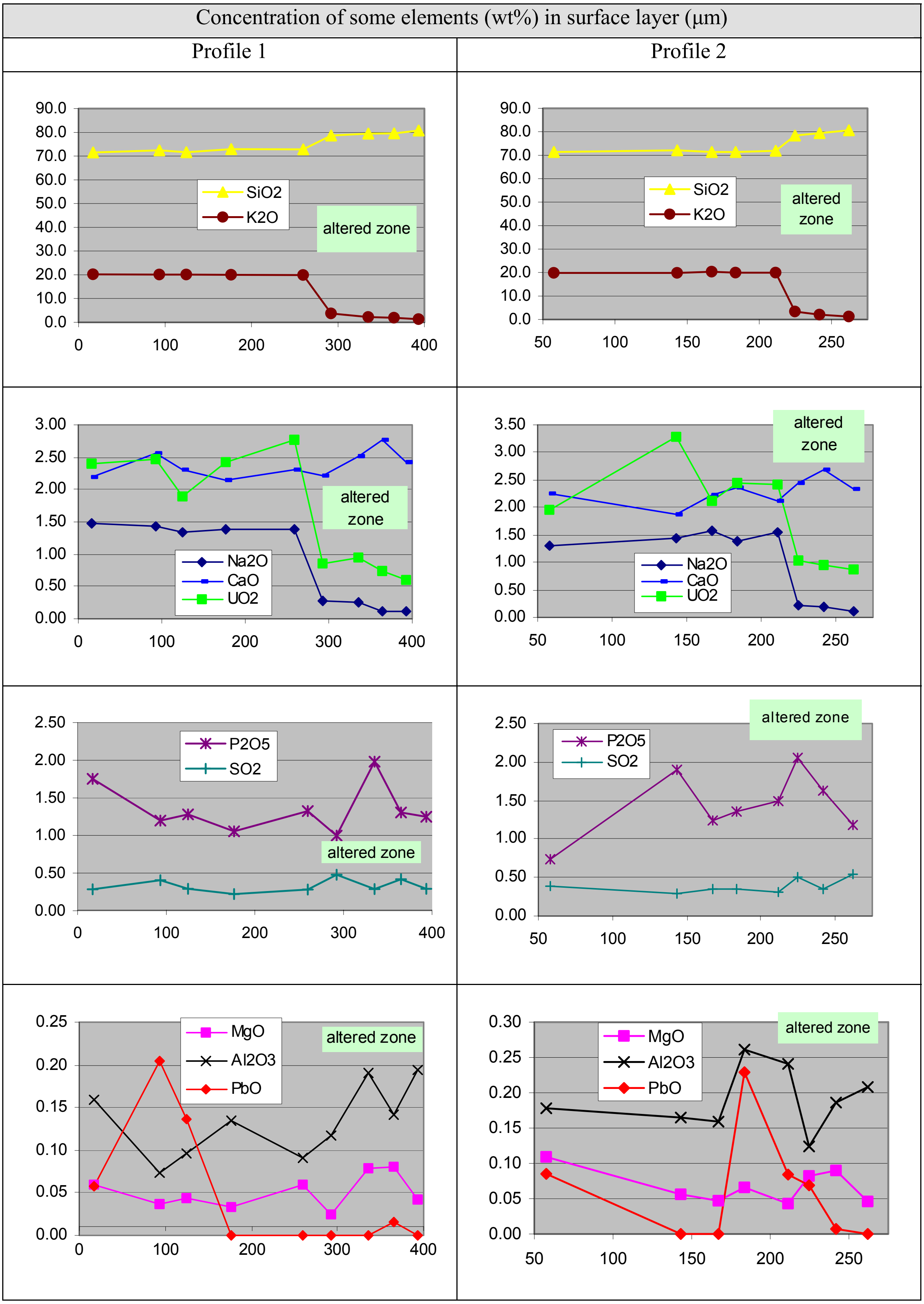

FIG. C–17. Concentration profiles of elements across altered zone to the relatively unaltered glass matrix.

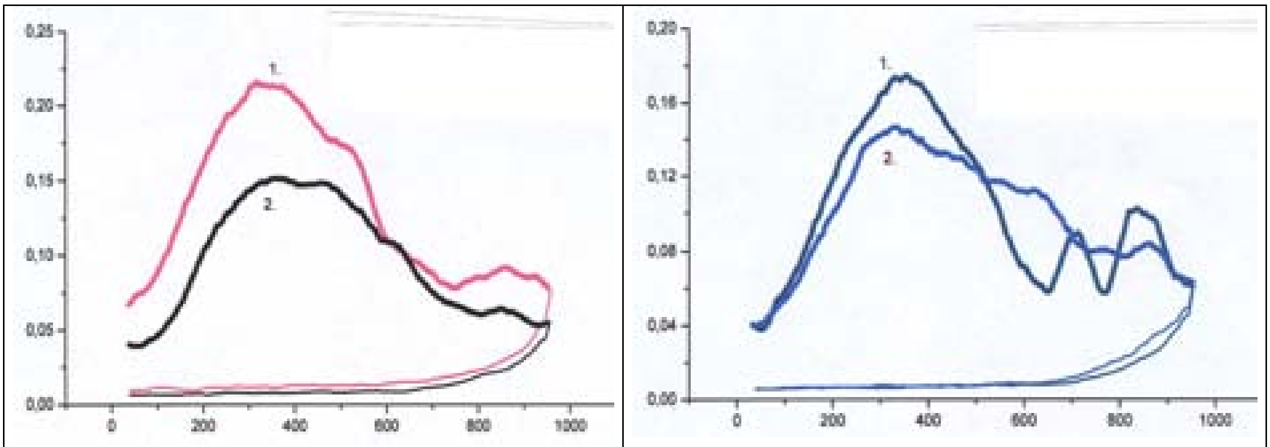

temperature

1. fresh surface - immediate measurement
2. altered surface - - immediate measurement

temperature

1. fresh surface - measurement after 5.5 months
2. altered surface - measurement after 5.5 months

FIG. C–18. ETA spectra measured on altered and unaltered samples.

5.2. Concrete material

The concrete walls of the basins are in permanent contact with highly radioactive water pumped from various springs. The content of interesting radionuclides is shown in the Table C–III.

TABLE C–III. THE CONTENT OF SELECTED RADIONUCLIDES AND URANIUM IN SPRINGS

Mine spring	**Ra–226** (kBq/l)	**Rn–222** (kBq/l)	**U** (mg/l)	**Pb–210** (mBq/l)	**Po–210** (mBq/l)
Behounek	12.3	6.5 – 12.8	0.084	542	45
Curie	2.4	3.3 – 6.3	0.011	825	77
C1	3.4	4.3 – 14.4	0.013	946	241

The floor of basins is covered by mud where various radionuclides are sorbed. The composition of mud is shown in the Table C-IV.

TABLE C-IV. THE ACTIVITY OF SELECTED RADIONUCLIDES IN MUD (Bq/kg)

	U–238 chain					**Th–232 chain**		**U–235 chain**		
	Th-234	**Ra-226**	**Pb-214**	**Pb-210**	**Bi-214**	**Ac-228**	**Ra-224**	**Th-231**	**Ra-223**	**Bi-211**
SJ	<9.7×10^3	2.3×10^6	3.0×10^5	1.8×10^5	3.3×10^5	4.8×10^3	3.3×10^4	2.7×10^3	<1.1×10^3	1.7×10^5
NJ	1.2×10^4	2.4×10^6	8.0×10^5	1.3×10^5	8.0×10^5	7.4×10^3	5.8×10^4	4.7×10^4	<3.1×10^3	5.1×10^5

Porosity, related parameters and analyses of the cement are shown in Tables C–V to C-VIII.

TABLE C–V. POROSITY AND RELATED PARAMETERS

Sample	**Total intrusion volume** (cm^3/g)	**Max. pore diameter** (nm)	**Porosity ε**
SJ–1	0.1021	10 - 90	0.26
SJ–4	0.0634	5 - 110	0.15
NJ–1	0.0789	20 - 70	0.18
NJ–4	0.0831	20 - 90	0.19

TABLE C–VI. ELEMENTAL ANALYSIS OF CONCRETE MATRIX (% wt, RECALCULATED TO DRY RESIDUE, 105°C)

Sample	**SJ–1**	**SJ–4**	**NJ–1**	**NJ–4**
Moisture (105^{0}C)	2.35	1.95	1.48	2.20
Loss by ignition (1,050^{0}C)	7.35	6.68	5.63	5.16
SiO_2	37.86	37.18	78.28	79.71
Al_2O_3	10.53	11.01	3.41	2.96
Fe_2O_3 (total)	11.73	12.43	1.05	0.75
TiO_2	4.11	4.51	0.38	0.29
CaO	15.07	16.80	8.18	8.24
MgO	9.53	7.45	0.81	0.62
Na_2O	1.61	1.52	0.14	0.08
K_2O	0.45	0.64	0.50	0.41
MnO	0.174	0.168	0.043	0.034
P_2O_5	0.72	0.79	0.11	0.07
SO_3 (total)	0.04	0.07	0.61	0.85

TABLE C–VII. DETERMINATION OF Th AND U IN CONCRETE MATRIX BY ICP–MS

	Sample							
	SJ–1	**SJ–2**	**SJ–3**	**SJ–4**	**NJ–1**	**NJ–2**	**NJ–3**	**NJ–4**
U (ppb)	15.55	14.52	4.49	20.10	3.58	8.08	1.85	1.84
RSD (at%)	19.9	12.0	12.0	12.0	12.0	12.0	12.0	12.0
Th (ppb)	0.3	4.2	3.0	0.2	2.6	0.5	0.3	0.3
RSD (at%)	12.0	12.0	12.0	12.0	12.0	53.9	38.8	13.1

TABLE C–VIII. SEMI–QUANTITATIVE DETERMINATION OF MINERAL PHASES BY RTG (NUMBER OF CROSSES INDICATES RELATIVE RATIO OF MINERALS +++ = THE HIGHEST AMOUNT)

Mineral	Composition	SJ–1	SJ–2	NJ–1	NJ–4
Quartz	SiO_2	+++	+++	+++	+++
Calcite	$CaCO_3$	++	+	++	++
Gypsum	$CaSO_4.2H_2O$	-	-	+	+
Ettringite	$Ca_6Al_2[(OH)_4(SO)_4]_3.H_2O$	+	+	+	++
Portlandite	$Ca(OH)_2$	-	-	+	++
Microcline	$KAlSi_3O_8$	-	-	++	+
Kaolinite	$Al_4[(OH)_8Si_4O]_{10}$	+	+	+	-
Muscovite	$KAl_2[(OH,F)_2AlSi_3O_8]$	++	++	++	++
Analcime	$NaAlSi_2O_6.H_2O$	++	++	-	-
Spinel – magnetite	Al_2MgO_4 - Fe_3O_4	++	++	-	-
Nepheline	$KNa_3(AlSiO_4)_4$	++	++	-	-
Siderite	$FeCO_3$	+	+	-	-
Augite	$(Ca, Mg, Fe, Ti, Al)_2[(Si, Al)_2O_6]$	++	++	-	-
Smectite – montmorillonite	$Al_{1.67}Mg_{0.33}[(OH)_2Si_4O_{10}]Na_3(H_2O)_4$	+	++	-	-

Analysis of selected parameters (mainly cations) in leachates from short-term leaching tests (HCl, pH = 3) are shown in the Table C–IX. Results for anions, neutralization capacities and derived parameters (carbonate forms) had unacceptable uncertainties not allowing the use of data for further interpretations and speciation calculations.

6. DISCUSSION

6.1. Uranium glass

Uranium glass was deposited in a close distance from the glassworks during production of glass. Other types of glass were prevalent — it is estimated that the uranium glass formed only the several percent of the whole volume/mass of glass deposited there. The precise conditions of deposition are not known. It can also be assumed that other unsuitable and unused material was deposited there from time to time, including material from the glassworks (slag), building material, soil, vegetation, etc. Also, periodic partial covering can be supposed to have occurred. Layers with higher content of uranium glass can be detected by beta/gamma spectrometry or by fluorescence indication.

TABLE C–IX. CONCENTRATION OF SELECTED ELEMENTS IN LEACHATES (mg/L) AFTER VARIOUS TIME PERIODS OF LEACHING

Time (days)	**Sample**	**Ca**	**Al**	**Fe**	**K**	**Na**	**SiO$_2$**
1	SJ–1	88	3.1	0.5	12	42	18
	SJ–3	140	9.3	2.2	9.5	10	21
	NJ–1	170	4.2	1.5	5.4	7.7	22
	NJ–3	610	0.7	0.2	6.0	4.3	1.7
4	SJ–1	69	3.9	0.5	6.6	11	19
	SJ–3	110	6.6	0.5	5.7	3.7	4.2
	NJ–1	220	9.0	5.0	2.9	1.4	49
	NJ–3	320	1.7	0.4	2.7	1.0	5.3
7	SJ–1	55	2.6	0.2	5.7	9.0	15
	SJ–3	290	1.3	0.1	2.2	0.9	1.6
	NJ–1	160	3.2	0.2	2.6	1.1	12
	NJ–3	110	5.6	0.1	5.1	3.7	7.4
39	SJ–1	90	8.5	4.7	5.2	8.4	38
	SJ–3	120	5.5	0.1	8.5	10	6.8
	NJ–1	140	2.3	0.4	5.3	2.2	6.8
	NJ–3	230	1.7	0.4	4.0	1.5	5.4

Mechanical corrosion and leaching of glass formed a typical aureole of higher concentration of uranium (2 mm soil fraction) — the concentration has reached tens of ppm of U (in two peaks at 0.4–0.8 m and around 1.5 m below the surface). Such relatively high mobility of uranium is typical for oxidizing conditions. Two similar accumulation peaks also occur for As and Pb in acetic acid soil leachates [19] and can be presumed for other metals used for glass colouring. The pattern of Ra-226 is not so straightforward, since it does not form an accumulation maximum, but is rather dispersed over 1 m below the surface. Radium is fairly well correlated with thorium. The range of pH in the soil leachate is typical for such soil-like materials in landfill. The peaks of pH (7–7.5) are fairly well correlated with concentrations of uranium.

The landfill is situated in the unsaturated zone, but the nearby local river can cause flooding to reach the landfill, as was documented during the summer of 2002. The mean annual precipitation at the nearest meteorological station (Primda) is a representative value for the study site (698 mm).

The uranium glass matrix is inhomogeneous, with frequent bubbles and spherical formations (Figure C–7) generally in two dimensions — smaller with diameter of several μm and larger with tens of μm. The characteristics of such formations are not fully understood — they can be composed of air or glass differentiates (product of glass melting or transformations) or helium/radon (accumulation of alpha decay products and daughter isotopes) if uranium can form local accumulations. Helium accumulation can be assumed from the disturbed character of some bubbles that could occur after exceeding some limiting pressure. The bubbles and similar formations need to by characterized using fluid inclusion studies used in geology.

ETA measurements revealed differences between the behaviour of fresh samples and samples with alteration layers. The mobility of radon in the superficial zone is similar in both cases (increasing part of curves) and differences occurred in the decreasing part of the curve that may indicate the role of different processes or the impact of different microstructure during radon release.

Relatively thick alteration layers were formed on the uranium glass samples (around 100 μm and thickness up to 600 μm is documented from samples from the same study site in [19]. Such thickness is typical for glass after longer interaction with clay or a natural soil environment. Based on representative thickness of alteration layers in the range of 100–500 μm originated over about 80 years (with assumption of time invariant corrosion rate and without important removal of material from the surface), the corrosion rate is 1.25–6.25 μm/a. The identified leaching of alkali from the altered layer is at usual level for this type of glass. PIXE and RBS measurements indicate approximately ten-fold enrichment of uranium in surface layers (0.5 μm) in comparison with the glass matrix (found in two samples). The microprobe profiles indicate clear depletion of uranium in the altered zone - below the RBS measurement sensitivity. The surface enrichment of uranium found on two samples remains unexplained to date. Possible explanations can be sorption (or co-precipitation) on the surface altered layer of glass and/or a manufacturing cause.

The derived corrosion rates are not possible to compare straightforwardly with corrosion/dissolution rates of other types of natural glasses or with the results from laboratory experiments with borosilicate glass. Dissolution of glass is complicated process depending on temperature, water/glass ratio, interaction time, and chemistry of solution and flow conditions. The derived corrosion rates of basaltic glass from various deposition environments (pelites, marine sediments, etc.) are reported at the level of tens to thousands of μm/1000 years. Higher corrosion rates found in Klastersky Mlyn samples can be (at least partially) explained by deposition in the high reactivity surface environment (influence of humidity, percolation, organic matter, etc.) in spite of high SiO_2 content indicating the relative resistivity.

6.2. Concrete material

The character of samples studied from old and new basins was different, mainly concerning the clastic phase used (coarser basic rock and finer quartz and feldspar sand, respectively). The porosity of the samples of concrete studied is around 20% without any clear trend. Table C-V shows that porosity is more evenly distributed in new than in old concrete samples. More uniformity can be found in the new concrete, whereas the old concrete exhibits the lowest intrusion volume. The measured porosity represents microporosity; in addition the older concrete contains macroporosity (cavities).

The results of the silicate analysis (Table C–VI) reflect different composition of concrete samples: in new concrete it was not possible to separate finer quartz and feldspar grains. The content of the main components (as totals) was not altered, even after long contact of these concretes with water, because the values obtained are independent of location of sampling (1 to 4 positions). After recalculation of the silicate analysis of younger concrete to a similar SiO_2 content as the older concrete, it has been revealed that the content of Fe is 3–4 times lower and the content of Ca and S (consistent with identification of gypsum) is higher in comparison with older concrete. Tens of elemental EDS analyses revealed high inhomogeneity of the samples, but afore mentioned findings are consistent with semi-quantitative RTG identification of mineral phases. RTG determination showed the different character of the concrete matrix - younger samples contain gypsum and portlandite (which the older samples do not contain) and, on the other hand, the older samples contain analcime, spinel/magnetite, nepheline and smectite phases. Such differences reflect their different ages (phase transformations toward more thermodynamically stabile minerals), but can also reflect differences in the composition of the cement paste.

Concentrations of U and Th determined in the analysed concrete matrices are in good agreement with the expectations. Both materials exhibit higher values of both elements in the concrete layers in contact with water, or close to this contact, than in layers which are farther from the water. These layers show differences of three in uranium content in both new and old concrete, and 5 to 2 in thorium content in new and old concretes, respectively. The quantitative evaluation for Th is rather inaccurate, as the total Th content in these materials is very low, even in comparison with the uranium content.

Accelerated shorter-term leaching experiments (HCl, pH = 3) provided only partially satisfactory results. Immense pH buffer capacity was found irrespective of age of sample or sampling position. Almost constant pH near 12 indicates buffering mainly by portlandite with transition to CSH phases (in older concrete). Such hyperalkaline environment is positive for immobilization and retardation of radionuclides by precipitation, co-precipitation and absorption (diffusion into the bulk material after surface sorption). Unfortunately, determination of anions, neutralization capacities and derived parameters (carbonate forms) had unacceptable uncertainties not allowing the use of data for further interpretations and speciation calculations. The low content of uranium and thorium in the concrete matrix prevented reliable measurement of these radioelements in leachates and therefore it was not possible to derive concentration profiles as originally expected. Due to oxidizing conditions in leaching experiments, the prevalence of hydroxide complexes in solution can be anticipated (e.g. $U(OH)_5^-$ species) along with some portion of carbonate complexes (e.g. $UO_2(CO_3)_3^{4-}$) as indicated by occurrence inorganic carbon species in solution.

REFERENCES

[1] BOUSKA, V., et al., Natural Glasses, Academia, Prague (1987) (In Czech).

[2] LUTZE, W., WING, R., Radioactive Waste Forms for Future, North-Holland, Amsterdam (1988).

[3] BOUSKA, V., TOLAR, V., PACESOVA, M., LACIOK, A., Natural Glasses as Analogues to Assess the Long-term Stability of Some Artificial Glasses, Geologica Carpathica, Series Clays, 6, 2, 107 (1997).

[4] EWING, R., Natural Analogues - Analogues for Radioactive Waste Forms, Scientific Basis for Nuclear Waste Management I, 57 (1979).

[5] GRAMBOW, B., Source Term for Performance Assessment of HLW Glass and Spent Fuel as Waste Forms - Scientific Basis for Nuclear Waste Management, XXI, 141 (1998).

[6] GRAMBOW, B., MULLER, R., First-order Rate Law and the Role of Surface Layers in Glass Performance Assessment - Journal of Nuclear Materials, 298, 112 (2001).

[7] GRAMBOW, B., Remaining Uncertainties in Predicting Long-term Performance of Nuclear Waste Glass from Experiments - Scientific Basis for Nuclear Waste Management, XVII, 167 (1994).

[8] KAMEI, G., YUSA, Y., ARAI, T., A Natural Analogue of Nuclear Waste Glass in Compacted Bentonite — Applied Geochemistry, 12, 141 (2000).

[9] LEMMENS, K., The Effect of Clay on the Dissolution of Nuclear Waste Glass, Journal of Nuclear Materials, 298, 12 (2001).

[10] BIWER, B.M., SODERHOLM, L., GREEGOR, R.B., LYTLE, F.W., Uranium Speciation in Glass Corrosion Layers: an EXAFS Study, Scientific Basis for Nuclear Waste Management, XX, 229 (1997).

[11] COOPER, G. I., COX, G.A., The Aqueous Corrosion of Potash-lime-silica Glass in the Range 10-250 ^{0}C, Applied Geochemistry, 11, 511 (1996).

[12] JIANG, W., ROY, D.M., Ancient Analogues Concerning Stability and Durability of Cementitious Waste Form, Scientific Basis for Nuclear Waste Management, XVII, 335 (1994).

[13] MILLER, W., ALEXANDER, W., CHAPMAN, N., McKINLEY, I., SMELLIE, J., Geological Disposal of Radioactive Waste and Natural Analogues, Pergamon – Elsevier (2000).

[14] LAGERBLAD, B., TRAGARDH, J., Conceptual Model for Concrete Long Time Degradation in a Deep Nuclear Waste Repository, SKB TR 95-21 (1995).

[15] ENDKVIST, I., ALBINSSON, Y., ENDKVIST, W.J., The Long-term Stability of Cement - Leaching Tests, SKB TR 96-09 (1996).

[16] TRAGARDH, J., LAGERBLAD, B., Leaching of 90-year Old Concrete Mortar in Contact with Stagnant Water, SKB TR 98-11 (1998).

[17] LAGERBLAD, B., Leaching Performance of Concrete Based on Studies of Samples from Old Concrete Constructions, SKB TR 01-27 (2001).

[18] BALEK, V., BANBA, T., MALEK, Z., MITAMURA, H., VANCE, E.R., The Use of Thermal Analysis in the Characterisation of Nuclear Waste Forms and their Alteration Products, Proceedings of FAERI Conference (1999).

[19] PROCHAZKA, D., Natural Corrosion of Historical Glasses Coloured by Uranium, Diploma Thesis; Faculty of Natural Sciences, Charles University, Prague (2002).

ANNEX D

UKRAINE

THE STABILITY OF THE ANCIENT METAL AND GLASS FROM ARCHAEOLOGICAL SITES OF THE NORTHERN PRICHERNOMOR'E (UKRAINE) AND THEIR PHYSICAL AND CHEMICAL INTERACTIONS WITH THEIR BURIAL ENVIRONMENT

V. Manichev, L. Demchenko, B. Zlobenko, V. Kadoshnikov, L. Spasova
Institute of Environmental Geochemistry NAS of Ukraine, Kiev, Ukraine

Abstract

A study has been carried out regarding degradation processes occurring on glass, copper and bronze artefacts excavated from the ancient settlement sites of Kamenka and Olbiya (the North Coast of the Black Sea). Its goal was to perform scoping evaluation of long-term resistance of some materials considered for the use as engineered barriers in a geological repository (waste form, container). The geochemical environment was characterised by analysis of accompanying soil. A variety of methods were employed to characterize the physical-chemical properties of the samples, including spectrography, X ray diffractometry, X ray spectrometry, infrared spectrometry, optical microscopy, scanning electron microscopy, chemical, mineralogical, spectral, radiocarbon dating, etc. and other analytic techniques. The study has shown that, under hydration conditions (weathering), a superficial layer of complicated structure was formed on the glass surface independent on glass composition; the thickness of this film varied from several tens to hundreds microns. The samples of ancient glass which contained organic substances showed the highest degree of alteration/degradation, but the reasons have not been revealed. It could be concluded that among the metallic ancient anthropogenic analogues of materials the most suitable were pure copper and low-tin bronzes (especially if subjected to mechanical-thermal treatment, such as cold and hot forging); however, their performance was significantly dependent on the geochemical conditions of the environment. Among the cast metals, the high-tin bronzes were the most corrosion-resistant, probably due to formation of thin protective film of oxidative phase on its surface.

1. INTRODUCTION

For many industrially developed countries, the problem of the disposal of radioactive waste (RAW) generated by the nuclear power industry and the interrelated long-term protection of the environment are important prerequisites for the further development of the nuclear industry. Currently, in the Ukraine, the strategy debated for the disposal of spent fuel and high level RAW in a geological repository (constructed in crystalline rocks) envisages the use of engineered multi-barrier systems. Worldwide, the geological disposal of vitrified RAW is considered to be a safe solution. The main problem of proving the safety of such repositories is the temporal factor. The long-term disposal of high level/long lived RAW requires extremely prolonged isolation of such wastes, far exceeding the reasonable limits of administrative control of such sites. Obviously, the problem of long-term glass dissolution and consequential release of radionuclides from vitrified RAW into a repository system requires detailed understanding of the time-induced changes in the physico-chemical properties of such glass (and its environment) during prolonged isolation of RAW. Study of the long-term stability of certain ancient artefacts, such as glass and metals (as material analogues for the vitrified RAW and engineered barriers), could provide important scientific and, to a certain degree, practical information.

Archaeological monuments in the northern part of the Black Sea Coast represent the remains of the ancient Greek settlements which existed in the beginning of the first millennium B.C. In the course of field expeditions (1999–2002), the authors collected a variety of glass and metal artefacts (together with accompanying materials/artefacts) from the different cultural soil layers of these archaeological sites. The comparative studies of the time-induced alteration of the physical and chemical properties of samples of archaeological glasses and metals were the subjects of the current research.

A variety of bronze and especially copper artefacts that were found in ancient soil layers were investigated for their corrosion behaviour, because copper is considered as one of the most promising materials for containers for high level radioactive waste [1–4]. Certain important aspects of long-term copper corrosion could be better predicted and understood via such investigations of archaeological artefacts.

However, it should be noted that the chemical compositions of the artefacts, and their interactions with the environment in which they were found, could not be totally comparable to the geochemical conditions of the modern repository or to the proposed modern repository materials.

2. LOCATION OF THE SITE

In the course of archaeological excavations of the historic monuments on the North Coast of the Black Sea — the ancient settlement sites of Kamenka and Olbiya — the authors collected multiple samples of archaeological artefacts such as copper, bronze, and glass, together with samples of the soil accommodating them.

The ancient city of Olbiya (town of Parutino, Nikolayev region) was settled by Greek colonists in the second quarter of the 6th century BC on the right bank of the Yuzhnyi Bug river near the Dnepr river estuary (Figure D–1/a). It was one of the three biggest ancient city-states on the North Coast of the Black Sea. The location of Olbiya was identified at the end of the 18th century and occasional excavations began here in the middle of the 19th century, but methodical excavations have been conducted only since 1901. In recent years, archaeological work has been carried out in the south–eastern part of the Upper Town (Sector R–25) along the slope towards the estuary.

The upper excavation site is located at 45 m, the middle at about 25 m and the lower about 10 m over the present Yuzhnyi Bug estuary level. The samples of ancient glass, copper and bronze artefacts were collected at the middle (Figure D–1/b) and lower excavation sites. Most of the upper town is located at the surface of a loess plateau, covered by liver-coloured solonetzic soil. The thickness of the Quaternary deposits was 20 m, including the humic horizon of 25–50 cm. Inter-stratification of loess, loamy soil and cultural layer soil is pronounced in the modern excavation site profiles.

The Kamenka town site is a monument of Scythian settled culture (4th–3rd century BC) located on the left bank of Dnepr near the modern town of Kamenka-Dneprovskaja, Zaporozhje region (Figure D–1/c). The town site occupies an area of about 12 km^2 and is situated on a dune cape. Two thirds of the archaeological monument's area are currently flooded by the Kakhovka Water Reservoir. Excavation of the site began in 1899–1900; later works were conducted in 1938–1950 [5] and in 1987–1993 [6].

The soils of the Kamenka town site are mostly composed of sand and silty river drifts and the site is periodically subject to spring floods because it is located at the river water level [6]. The cultural layer at the sampling points consists of dark grey, almost black, 0.8–1.2 m thick soil similar to the mainland soil (Figure D–1/d) and is covered by 0.5–0.7 m thick light and grey sands.

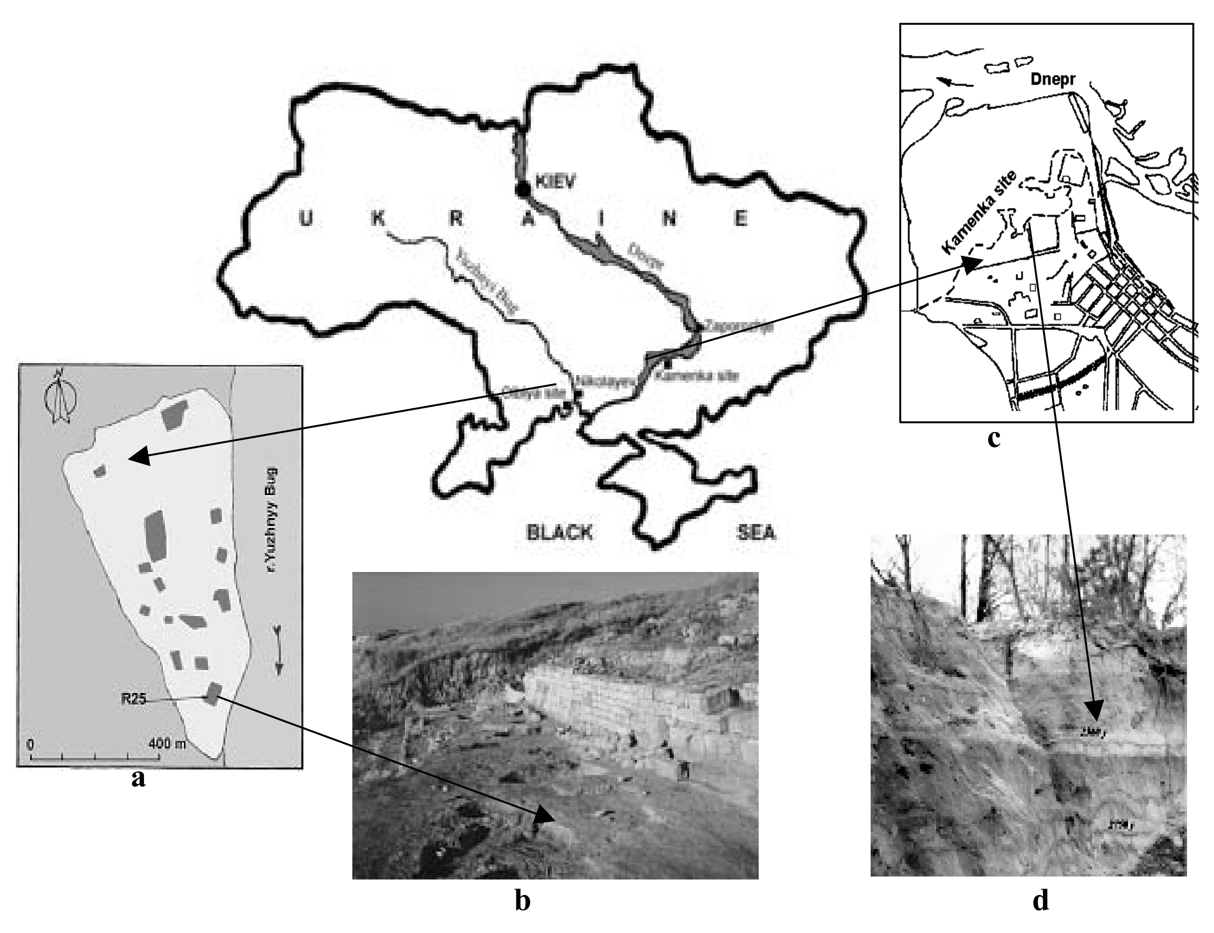

FIG. D–1. Schematic map of the Ukraine showing the location of the archaeological monuments – the ancient settlement sites of Kamenka and Olbiya:

- *(a) schematic map of Olbiya, showing the excavation sites;*
- *(b) general view of the Olbiya excavation site;*
- *(c) schematic map of the Kamenka site;*
- *(d) general view of the cultural layer at the sampling points.*

According to the paleochronological soil analysis data, the climate in this region changed from cold arid to hot arid [7]. At present, the area is represented by step landscapes, the climate is predominantly continental, the average annual temperature varies between 8-11°C and the amount of precipitation varies over the territory between 320-370 mm/year [8].

3. GEOCHEMICAL CHARACTERISTICS OF EXCAVATED SOILS

Soil samples collected from cultural layers of the Olbiya and Kamenka ancient sites were dated by radiocarbon chronometry. Micro-chronometry of soil, by methods established by the authors [9], confirmed that Olbiya could be dated to the first century BC and artefacts from the Kamenka site to the 4th century AD.

It should be noted that chemical composition and specific properties of soils, such as pH and buffer capacity, have been changing with time, and, at present, both climate and the soil reactivity on the site are different. Thus, in order to define the real influence of archaeological soil conditions on the corrosion process, it is necessary to study the time evolution of the soil characteristics, such as decalcification and modification of the buffering capacity of the soils.

The presence of sulphates, chlorides, organics and carbonate carbon in soil influenced the corrosion of the artefacts buried in it. Chemical aggressiveness of the soils was studied by determining the pH and Eh of the water and salt extracts by standard techniques (Table D–1). The data demonstrate that the presence of increased amounts of organic substances in the Olbiya soil promoted the change of oxidation-reduction potential, thus strengthening reduction properties and, accordingly, decreasing the Eh.

TABLE D–I. GEOCHEMICAL CHARACTERISTICS OF THE SOILS

Site of soil sampling	**Element content** (%)					**pH**		**Eh** (mV)
	P_2O_5	**S**	**Cl**	**$C_{org.}$**	**C_{carb}**	**Water extract**	**Salt extract**	**Water extract**
Kamenka	0.05	0.02	0.12	0.8	0.13	8.0	7.4	+200
Olbiya	0.42	0.05	0.19	1.10	1.60	8.6	8.2	+160

The data in Table D–I indicate that, compared to the soil of the Kamenka ancient town site, the Olbiya soil contains slightly more sulphur and chlorine and significantly more organic substances, including organic and carbonate carbon. The presence of carbonate carbon caused significantly higher alkaline soil solutions.

The mineral composition of the soils and presence of organic matter were the most important factors influencing the copper corrosion rate. As illustrated in the work [10], change of the soil pH depends on both calcium carbonate content in infiltrating ground water and the presence of calcite (as a buffer of pH). An increase in CO_2 partial pressure will increase the dissolution rate of calcite, gypsum or anhydrite, pyrite oxidation and anaerobic oxidation of organic matter, thus resulting in accelerated copper corrosion (Table D–II).

TABLE D–II. MINERAL COMPOSITION OF SOIL

Site of sampling of soil	**Mineral composition of soil fractions**		
	Sand fractions >0.1 mm	**Silt fractions** 0.001–0.1 mm	**Clay fractions** <0.001 mm
Kamenka	quartz, feldspar,	quartz, feldspar,	hydromica, kaolinite, quartz
Olbiya	quartz, feldspar, calcite, dolomite, gypsum,	quartz, feldspar, calcite, dolomite, gypsum,	hydromica, kaolinite, quartz

Organic matter, calcite and gypsum, which are present in the Olbiya loess loams (but not in the Kamenka ancient town site soil), could interact with water, thus promoting an acceleration of copper corrosion. As we mentioned, the chemical composition and reactive properties (pH, buffer capacity) of the surrounding soils (archaeological layers where all artefacts were found) have been changing throughout time. Therefore, in order to define a real meaning for archaeological soil conditions as related to corrosion, it is necessary to consider the soil micro-morphology to determine the time evolution of the soil characteristics such as decalcification and modification of the buffering capacity.

4. MATERIAL STUDIED

The samples of ancient materials (metal, glass) from archaeological sites in the Northern Prichernomor'a (Ukraine), dated to the first and third century AD, were investigated for their susceptibility to soil corrosion. All glass samples were collected together with the surrounding soil samples and preserved in thick plastic bags.

A variety of glass samples (small pieces and tableware fragments) were excavated or collected at the ancient settlements and also at burial sites in Olbiya and other ancient cities. The ancient glass collection was represented by samples of colourless glass and samples of light-blue and greenish glass. The sizes of the pieces varied from 1–6 cm**.** Glass pieces from all cultural layers showed different degrees of corrosion, as indicated by silvery films on their surface and/or by bright iridescent colours. The degree of alteration of the glass debris was determined by their chemical composition, their location in the soil and the soil type. Three glass samples with different degrees of alteration, all collected from the same soil horizon, were selected for detailed investigation:

- ***Glass sample SP–132/17*** This sample (dated I AD) was represented by a ~4.5 mm thick, slightly bent, light-blue, and transparent glass splinter (Figure D–2). The main part of the external plane (80–90%) was greatly altered, but unaltered relic glass parts could also be observed. The external glass layer was of blue-white colour with mother-of-pearl lustre. An altered plane layer was weakly connected with the main unaltered glass part and could be easily exfoliated under slight mechanical pressure.
- ***Glass sample SP–149/21*** This glass sample was triangular in shape, transparent, colourless and ~ 0.75 mm thick (Figure D–3) and was dated II AD. The surface layer of this glass sample was greatly altered and appeared as white, with mother-of-pearl lustre.
- ***Glass sample SP–164/1*** This glass sample was represented by a transparent splinter of bluish colour and was dated II A.D (Figure D–4). Multiple single spheroids (~80 µm), as well as their aggregations, could be observed on the external glass surface. Black inclusions of organic matter were present either in the centre of spheroids, or forming elongated concentric zones in spheroids

In addition to ancient glass samples, a collection of metal artefacts manufactured from copper and bronze was found in the middle site (from soils of I–III A.D). Most of the metal artefacts were represented by high-tin content bronze, but some ingots of relatively pure copper and samples of bronze with high lead content were also found. Three copper artefacts from the Olbiya archaeological site collection were selected for detailed studies of time-induced structural alterations. Samples were cut in carefully selected directions (as shown in Figure D–5) and cut-off surfaces were thoroughly polished.

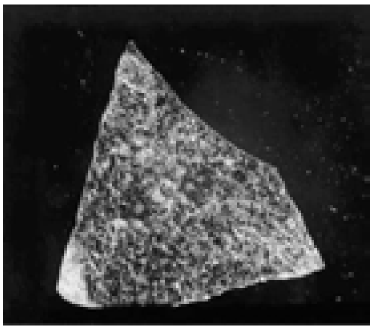

FIG. D-2. Glass sample (SP-132/17, ×2).

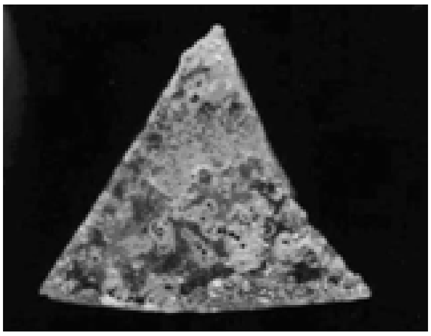

FIG. D-3. Glass sample (SP-149/21, ×2).

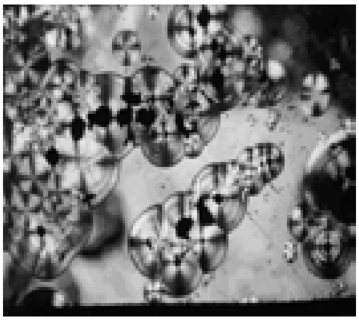

FIG. D-4. Thin glass section in transmission polarization light (glass sample SP-164/1, × 250,crossed nicols).

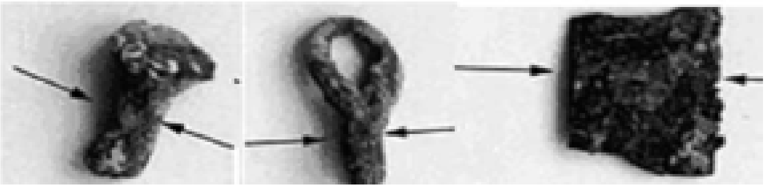

1 – nail 2 – wire-loop 3 – plate

FIG. D–5. Copper artefacts from Olbiya.

Likewise the ancient metal artefacts that were found in the Kamenka site (Figure D–6) the Olbiya site (Figure D–7) findings were also represented by copper-based alloys with various contents of Sn, Pb, and some other impurities.

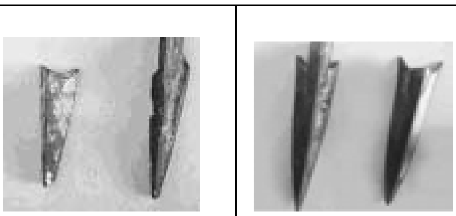

5- red/brown arrows 6 - black arrows

FIG. D–6. Bronze artefacts (Kamenka site).

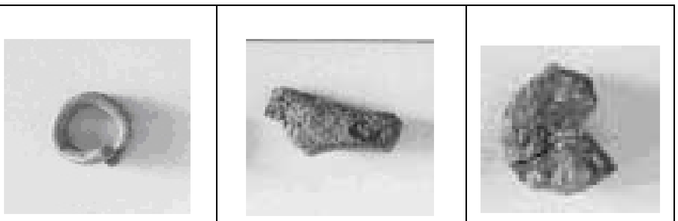

7 - wire ring 8 - plate-dolphin 9 - coin

FIG. D–7. Bronze artefacts (Olbiya site).

This representative variety of samples/artefacts that were collected at different archaeological sites provided a unique opportunity to study the degree of corrosion stability of samples that were altered under identical geochemical conditions.

5. ANALYTICAL METHODS

A variety of analytical techniques were employed for detailed study of the physical-chemical and physical properties of the samples of ancient glasses and bronzes including:

- Spectrograph CTE–1 (half-quantitative spectral analysis);
- Diffractometer DRON–UM–1 (x ray powder diffraction);
- Spectrometer VPA–30 (x ray fluorescent analysis);
- Spectrometer JXA–5 (x ray microanalysis);
- Spectrometer UR–20 (400–4000 cm^{-1} — infrared transmission spectra for testing ancient glass samples.

Detailed mineralogical and metallographic studies of the samples of ancient metals (cut and polished sections of a cylindrical body) were carried out by using optical microscopy and scanning electron microscopy. Samples of the surrounding soil were analysed by a variety of chemical, mineralogical, spectral, radiocarbon dating and other analytic techniques. Water samples extracted from the surrounding soil samples were analysed for pH and Eh.

6. EXPERIMENTAL DETAILS AND DISCUSSION

6.1. Archaeological glass

Study of the samples of archaeological glass could be very informative with respect to the mechanisms of long-term stability of the vitrified matrix proposed for solidification of HLW, which is also similar to the general mechanisms of weathering of silicate glasses. For example, the character of SON 6818 or RT-17 glass alteration is known to differ little from that of typical silicate glass [11]. All the ancient glasses that were studied in our laboratory are typical silicate glasses.

The comparative analysis of the archaeological glasses testifies that within even one archaeological monument, in the same soil type, on the same stratigraphic level, it is possible to observe various degrees of glass alteration. This probably can be explained by the variation of local physical/chemical conditions in which the ancient glass samples were discarded. The morphology of ancient glasses was studied mostly by optical microscopy with an emphasis on studies of the surface film composition and appearance. Study of the surface layer composition revealed that large cations of Na and Ca, and partially Si were actively washed out into the environment, while aluminium was accumulated in the degraded surface layer. This is characteristic for processes of weathering of silicates and alumosilicates.

Degraded surface layers were characterised by pronounced lamellar and lamellar-porous structures. Their substantial composition was close to that of aluminium-silicon gels. IR-spectral analysis indicated that surface films on the ancient glasses contained considerable amount of adsorptively-bound water (decreasing from the periphery to the centre). The thickness of the film formed on the surface of the ancient glass was from several tens to hundreds of microns, but an attempt to link this thickness of the films with ancient glass composition was not conclusive. In the same cultural layer, samples of ancient glass with similar chemical composition were characterised by various degree of degradation and the thickness of the surface films differed more than an order of magnitude.

Infrared spectroscopy study of glass samples with different alteration rates was carried out with the main objective of studying the process of glass hydration. The specific infrared transmission spectra of these highly altered glass samples (Figure D-8) were obtained selectively for various parts of the sample as following:

- The separated superficial layer;
- The altered layer;
- The unaltered glass body obtained by grinding the matrix after removing the altered layers.

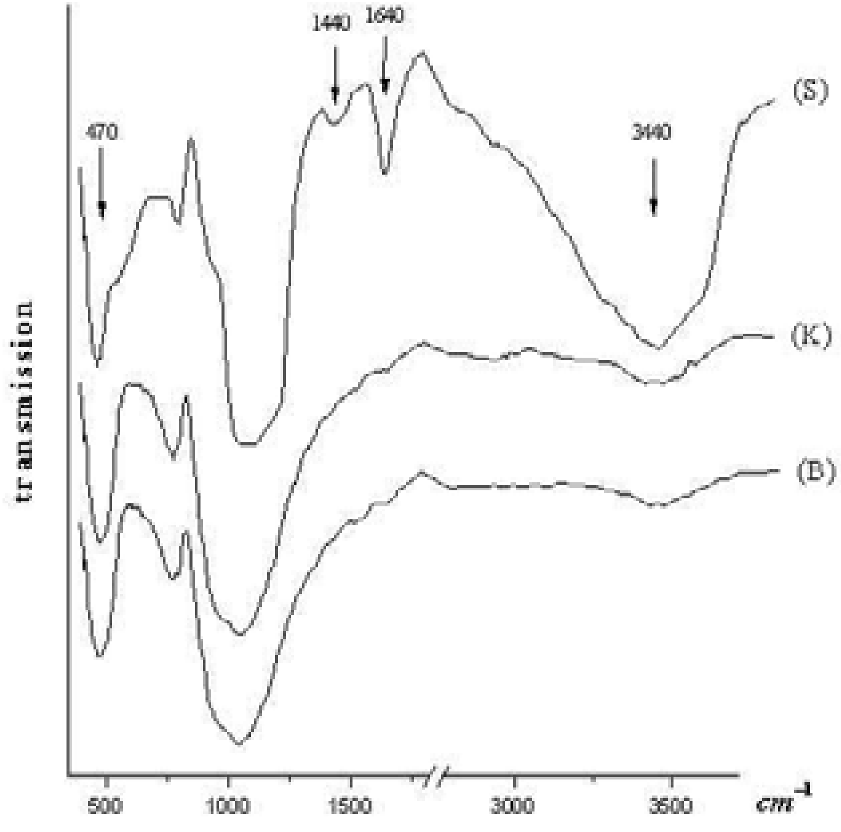

FIG. D–8. The infrared transmission spectrum of a sample of ancient glass:
(S) — the separated superficial layer;
(K) — the glass sample with the altered layer;
(B) — the unaltered glass part.

Using the thickness of the surface film as a factor of archaeological glass weathering, we can conclude that ancient glasses with similar degrees of degradation that were found in similar soils at the same stratigraphic level, have undergone throughout time comparable weathering processes, which were probably a consequence of the similar physico-chemical conditions imparted by the surrounding soil.

The external part of the altered layers was ~10–20 μm thick and increased to the centre of the samples and decreased to their peripheral parts. Brownish-brown organic matter was mainly located in the outside parts of the surface layer of the samples and was also more concentrated in the centre. Organic matter inclusions were also infrequently observed in the deeper layers of samples.

X ray phase analysis of the external surface layers showed the presence of crystalline phases, which were identified as aluminum foliated silicates of structural type 2:1 (hydromica, montmorillonite and calcium-bearing zeolite). As a rule, the samples of ancient glasses which contained organic substances indicated the highest degree of alteration/decay. The role of organic matter in this process is not entirely clear. Thus, more detailed studies of the influence of organic matter (including micro-organisms) on the rate of silicate glass alteration/decay should be carried out.

6.2. Corrosion of pure copper artefacts

Pure copper artefacts were found only during excavations in Olbiya. Three samples were taken from the collection for detailed study of the time-induced structural changes of the metal. Results of emission-spectral analysis of metal composition showed that all three artefacts were made of pure copper, with minor admixtures of Al, Ag, Mg, Si, Sn, and Pb.

The composition of corrosion products was studied by X ray spectral and diffractometric phase analyses. X ray diffractometric examination of the structure of the surface and near-surface metal layers, as well as its core, revealed the presence of minerals that are characteristic of the copper oxidation zone, such as cuprite, malachite, and covellite. The corrosion layer was practically completely mineralised; diffraction peaks of copper were very weak. Almost equal quantities of copper and cuprite, with admixtures of malachite, were present in the near-surface layer, while the core of sample showed only peaks of copper with minor admixture of cuprite. Table D–III presents the results of X ray microprobe analysis of the surface cross section of a copper sample taken along the radius from the centre to the surface.

TABLE D–III. X RAY SPECTRAL MICROANALYSIS OF CROSS SECTION SURFACE OF A COPPER SAMPLE

Sample section	**Elements** (%)							
	Cu	**Al**	**Si**	**Fe**	**Sn**	**Pb**	**Cl**	**C**
Core	99.038	0.206	0.201	0.041	0.077	0.137	0	0
Near surface	76.232	0.316	0.380	0,093	0.095	0.153	0	0
Surface	77.106	0.538	0.265	0.293	0.142	0.171	21.621	0.038

The data indicate that such elements as Cl, C, Fe, and Al, which are typical for the surrounding soil, were abundantly present in the surface layer (consisting mostly of corrosion products). The unaltered (metallic) copper content decreased from the centre of the sample to the periphery, thus indicating an increasing rate of mineralization of the metal sample.

Metallographic analysis of the pure copper samples studied established two distinct types of metal structures, probably as a result of different techniques used to manufacture the artefacts: casting and mechanical/thermal post-processing that was used to shape an artefact (see Figure D–9). On average, the central part of the cast sample (that was resistant to corrosion) was ~5.5–6.1 mm. The thickness of the corrosion layer, as measured along the radius to the periphery of sample, was non-uniform and ~1.4–2.3 mm. The structural conditions of two samples that were mechanically and thermally post-processed appeared to be more homogeneous than that of the cast samples. The corrosion layer of the wire loop sample was ~1.4 mm (unaltered metal core ~0.7–1.2 mm) and the corrosion layer of the un-riveted plate sample was ~0.26–0.32 mm (unaltered metal core ~2.8–3.1 mm).

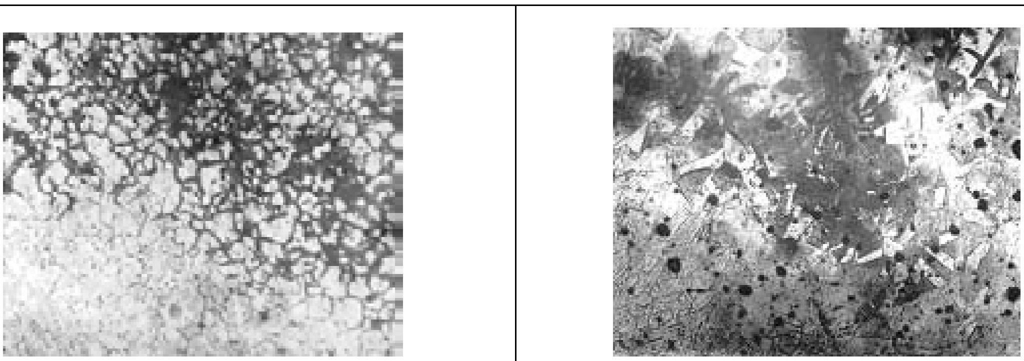

a – crystalline structure of cast sample (×70)

b – structure formed in the cast sample after mechanical/thermal treatment (×340)

FIG.D-9. Different types of structure of pure copper samples.

In the cast samples the grain size increased from the periphery to the centre and varied in the quite wide range from 40–95 μm. The grain boundaries were characterised by structural features that could be attributed to the casting of metal into the mould (probably a clay one) which was then followed by annealing. In this case, the external surface of the artefact is expected to be very rough. Therefore, for cast copper samples, an oxidation process resulting in the formation of mineralogical phases produced very non-uniformly altered surfaces. It was observed that corrosion started on the roughest parts of the surface and eventually penetrated deep into the sample along the grain boundaries, inflicting the most pronounced failures in crystalline lattice structure (Figure D–10).

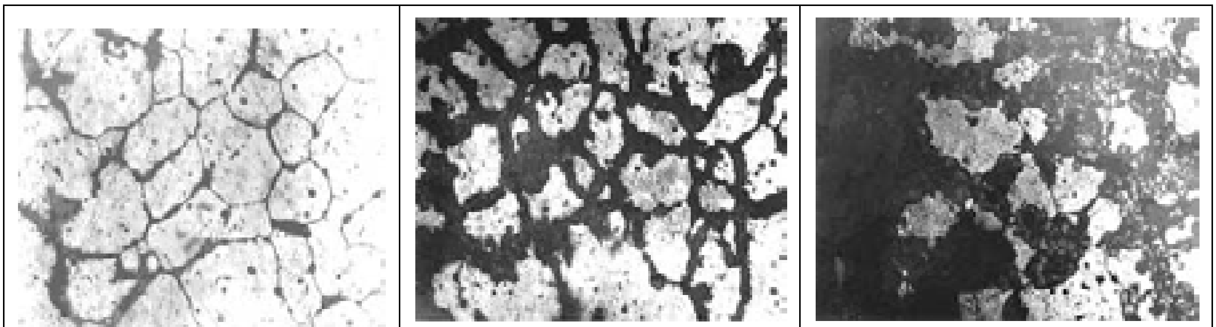

a – centre

b – subsurface layer

c – surface layer.

FIG. D–10. Corrosion penetration deep into cast copper sample (×340).

Hence, the obvious conclusion could be made that the corrosion process was mostly of an inter-crystalline character. The crystalline structure of metal of hardened samples (Figure D–9/b) was characterized by fine grains ~20–35μm, and also by the presence of twins (stretched unequal grains). The corrosion layer was also thinner and more uniform. These artefacts were most likely forged.

Study of the degree of corrosion susceptibility of the samples of pure copper that were found in the similar geochemical environment of Olbiya (but with a slightly different crystalline structure) revealed the following: the artefacts that underwent mechanical/thermal treatment after casting were more corrosion-prone than the cast one. The corrosion rates were 0.7–0.4 µm/a and 1.2 µm/a respectively.

6.3. Structural features and corrosion rate of bronze alloys

Some of the metal artefacts found at Olbiya and Kamenka were made of copper-based alloys with various percentages of Sn and Pb and other admixtures and could be classified as bronze. Table D–IV shows the content of the main alloying elements in the artefacts studied. The data show volumetric non-homogeneity of tin distribution in bronze alloys with high-tin content.

TABLE D–IV. VOLUMETRIC DISTRIBUTION OF ALLOYING ELEMENTS IN BRONZE ARTEFACTS (%)

Artefact No.		**Artefact specification and fragment studied**	**Cu**	**Sn**	**Pb**	**Si**
4	**Kamenka**	Spinner, cross-section	97.533	2.007	0.028	0.328
5		Red-brown arrows:				
		Intact facet	68.661	4.246	3.975	0.154
		Cross-section	74.810	20.343	3.152	0.261
		Cross-section	63.039	22.232	2.894	0.291
		Cross-section	64.380	25.834	2.842	0.190
		Cross-section	70.231	24.610	3.292	0.243
6		Black arrows:				
		Intact facet	17.038	56.408	4.649	2.094
		Intact facet	22.251	51.032	4.724	10.542
		Cross-section	70.760	24.164	4.059	0.479
		Cross-section	69.586	25.871	3.821	0.238
		Cross-section	71.229	24.848	3.708	0.207
		Polished facet	71.701	25.521	2.669	0.068
7		Ring, *cross-section of wire*	93.342	6.171	0.037	0.003
8	**Olbiya**	Plate “dolphin”, *cross-section*	95.466	4.103	0	0.006
9		Coin, *core of cross-section*	82.567	17.030	0.026	0.078
10		Combination of a metal drop with glass, *cross-section*	86.908	10.990	1.054	0.057

Thanks to the comprehensiveness of the collection of metal artefacts from various levels of the Olbiya and Kamenka sites, we were able to compare the level of corrosion susceptibility of bronze and copper alloys under similar geochemical conditions (Olbiya) and to study the influence of different geochemical environments on the corrosion of bronze alloys (Olbiya and Kamenka).

It was found that the tin bronze artefacts of ancient Olbiya were highly susceptible to corrosion. Metallographic analysis of a cross-section of the bronze plate —"dolphin" (No. 8) with tin content of 4% revealed the dendrite structure which is peculiar for casting. The plate was ~2.8–3.2 mm thick with a corrosion layer of ~0.3–0.9 mm. The 4.5–5.2 mm thick cast coin (No. 9) with tin content of 17% was almost completely mineralised. The lamellar structure of the cross-section of this sample is presented at Figure D–11.

The X ray diffraction picture of corrosion products revealed the presence of minerals of pseudo-malachite $Cu_5[PO_4]_2[OH]_4$, tenorite CuO, cuprite Cu_2O, andrewsite $(Cu,Fe)_3Fe_6[PO_4]_4[OH]_{12}$, and higginsite $CuCa[AsO_4][OH]$. Residue of the metal remained only in the core of coin (surrounded by cuprite with $CuClO_4$ and β-phase CuSn).

Artefact No. 10 was a metal drop joint with glass. The bronze composition of this artefact was different: 1% Pb and 11% Sn. The structure of metal was characterized by the presence of well-formed equilibrium grains with lead inclusions (eutectoid phase) that were distributed at the boundaries. The corrosion layer at the surface of the sample was heterogeneous and varied between 0.3–0.7 mm thick.

The results of the study of corrosion susceptibility of cast bronze and copper artefacts revealed that the thickness of corrosion layer for the majority of samples was nearly equal. Depending on the composition, the corrosion rate of tin bronze in some cases was higher than that of pure copper.

Ancient Scythian bronze of an earlier period was represented by objects No. 4–7 (Table D–IV), which were excavated from the archaeological monument of Kamenka. The geochemical and mineralogical characteristics of the soils composing the cultural layer (where the artefacts were found) were different from those of the Olbiya soil. Also, the bronze artefacts from these sites varied, both in tin content and in mode of manufacturing. After careful examination, all the bronze artefacts found were classified into four groups:

- Low-tin cast bronze Cu+2-4%Sn;
- Low-tin wrought bronze Cu+6%Sn;
- Medium-tin cast bronze Cu+11-17%Sn;
- High-tin cast bronze Cu+23-25%Sn.

The low-tin cast bronze was characterized by a dendritic structure with various degrees of dendrite branching depending on the cooling rate of the casts. Formation of minerals in the copper oxidation zone took place initially at the rough surface; the smoother sections were subjected to corrosion to a lesser extent. The corrosion layer thickness was inhomogeneous and varied from 0.2–0.5 mm to 0.7–0.9 mm. The corrosion rate was estimated to be in range of 0.11–0.41 µm/year.

By comparison with the modern classification of tin bronze for reformatted alloys [12], it follows that the ancient copper alloys with Sn content not exceeding 9% could be attributed to this class. Normally, semi-manufactured alloys with high corrosion resistance and mechanical properties could be manufactured by cold deformation of the original cast material after homogenizing annealing at 620°C. In our collection, only one sample of ancient analogues of bronze of such type (No. 7) was found at the excavation sites.

Metallographic analysis of alloy No. 7 (Figure D–12) revealed the characteristic features of a deformation structure of an α-solid solution and absence of phase components. The presence of re-crystallized grains and the directions of growth of boundaries of twins provided clear evidence of the original squeezing of the wire (that inflicted additional flexural strain) and intermediate annealing. Such an untypical example of ancient processing of tin bronze was found for the first time, since bronze artefacts were usually fabricated by casting. The thickness of the corrosion layer that was composed by cuprite, azurite and malachite was insignificant: ~50–70 μm; the corrosion rate was found to be 0.017–0.024 μm/a.

Medium-tin cast bronzes (No. 9 and 10) that were found at the Olbiya site were also highly corroded. The corrosion rate was estimated to be 0.33–1.91 μm/a.

Arrow-heads found in the Kamenka site were made of high-tin cast bronze. The surface of some of arrow-heads was covered with black patina and others with ginger-green patina. The arrow-heads of both types showed only insignificant degree of corrosion.

The X ray spectral analysis revealed that all arrow-heads were made of high-tin bronze (23–25% Sn) with 3–4% Pb admixture. The arrow-heads No. 6 were excavated in loess loams of the burial mound, while No. 5 was in sand soils of the Scythian settlement.

The X ray spectral microprobe analysis of the intact lateral surface of object № 6 and cross-section surface revealed that the tin content increased from the surface to the centre 4,2→17→22→27%.

Examination of the cross-sectional surface of the metal structure (Figure D-13) confirmed an enrichment of the casting core with tin, as a result of direct segregation during hardening. Such a picture normally could be observed during dendrite segregation, resulting in the gradient concentration of Sn. It could be explained by the fact that hardening of tin-leaden bronzes begins with isolation of copper-rich crystals of α-solid solution while the mother liquor becomes enriched with tin. In the course of time, a thin film of olive-brown patina (~30–40 μm) composed of copper oxidation products was formed on the surface of the sample. The X ray phase analysis of the intact surfaces of samples No. 6 and No. 7 shows that corrosion products were primarily composed of copper oxyhalogenides $CuCl_23Cu[OH]_2$, imparting a greenish colour to the sample. The time induced oxidation of these samples formed a corrosion layer ~30–60 μm thick.

A quite different picture was observed for the arrow-heads, which had very similar alloy composition but were covered with a black protective film. The X ray phase analysis of the intact lateral surface of sample No. 5 and of the cross-sectional surface showed that tin content decreased from the surface to the centre 56←26←24 %, which is typical for inverted segregation during hardening.

The thickness of the black protective film on the arrow-heads was determined by stage-micrometer (light microscopy), after polishing/etching of the various cross-sections, and was found to be in the range ~25–30 μm.

It is well known that the phenomenon of inverted segregation, sometimes called a “tin sweat”, is often observed on tin bronze castings, especially when these casting were manufactured by using sand-clay moulds. In such cases, Sn content in the “tin sweat” could be 2–2.5 times higher than the average content in the alloy [12].

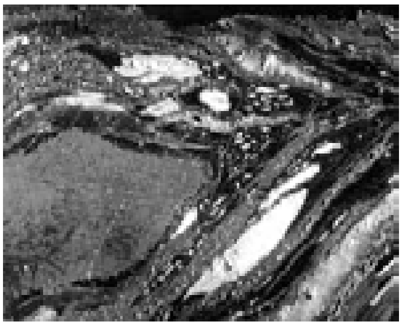

FIG. D-11. Mineralised surface of coin's cross-section (No. 9); Cu, with 17% Sn; corrosion layer ~3.7-4.5 mm.

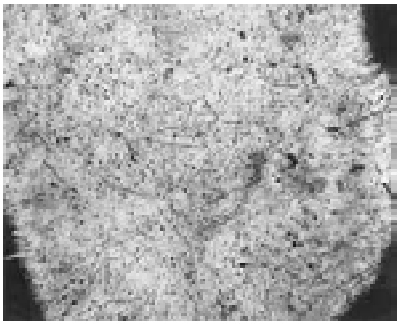

FIG. D-12. Cross-section structure of wire ring sample (No. 7); Cu with 6% Sn; corrosion layer ~50-70 µm.

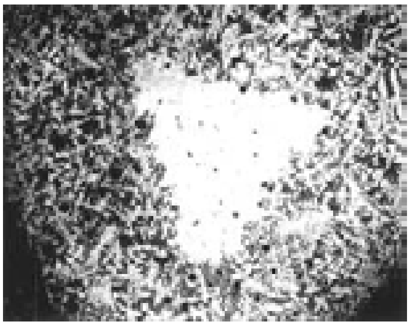

FIG. D-13. Cross-section structure of sample No. 2; Cu with 23% Sn and 3% Pb; corrosion layer ~30-40 µm.

The X ray micro-probe analysis of the intact surfaces revealed a considerable amount of Si, in addition to Sn and Pb (Table D–IV). It also revealed the peaks of ε-phase of Cu_3Sn and β-phase of Cu_8SiS_6 . Phase analysis of the polished surface indicated the presence of δ-phase of $Cu_{31}Sn_8$, Cu_2O, and Cu_4Si, SnO_2.

The metallographic study of cross-section surface of sample No. 5 revealed a chaotic distribution of phase inclusions ($Cu_{39}Sn_{11}$, $CuSiO_3$, Cu_8SiS_6, $PbCO_3$) over the sample, with predominant accumulation of them near to the external surface. Therefore, it was concluded that the corrosion resistance of high-tin bronze with inverted segregation during hardening was caused by the process of metal passivation, which could be described as formation of a thin protective phase film as a result of eutectoid transformation $\delta \leftrightarrow \alpha + \varepsilon$, which proceeds very slowly during the ageing of natural alloy.

Assuming the corrosion process to be uniform, and comparing the cultural epoch chronometric data and the thickness of the corrosion layer of artefacts (high-tin bronzes), we can conclude that the overall corrosion rate could be regarded as quite low. To a first degree of approximation, it was about 0.013–0.025 µm/year, which is an order of magnitude lower than the typical rate of an atmospheric corrosion of a modern tin bronze (Table D–V) [12].

Thus, in spite of the high corrosion resistance of high-tin bronzes, they are subject to brittle mechanical failure and do not stand shock and bending strain, which is an obstacle for the application of them as a material for radioactive waste containers. Table 6 presents results of the assessment of ancient metal corrosion rate by thickness of the corrosion layer formed during a certain period of time.

TABLE D–V. CORROSION RATE OF BRONZE ALLOYS IN DIFFERENT ENVIRONMENTS (mm/a)

Alloy	Sea atmosphere	Sea water	Rural area atmosphere	Urban area atmosphere
Cu	50	NA	NA	NA
Cu-Sn	1–2	5–76	0.15–0.8	1.5–1.8

As seen from Table D–VI, the Olbiya low-tin and medium-tin bronze had a similar corrosion rate, 0.14–0.33 µm/a, while the corrosion rate of article made from high-tin bronze was 1.43–1.90 µm/a. On the other hand high-tin cast bronzes found in loess-like loamy and sand soils of the Kamenka site had corrosion rate of 0.01–0.017 µm/a. The corrosion rate of low-tin bronze, subjected to mechanical thermal treatment after casting, was practically similar, i.e. 0.017–0.024 µm/a.

TABLE D–VI. CORROSION RATE OF ANCIENT METAL OF ANTHROPOGENIC ARTEFACTS

Site of sampling	**Age** (years)	**Type of soil**	**Metal composition**	**Way of artefact producing**	**Corrosion rate** (µm/a)
Olbiya	2100	Loess-like loamy soil	Cu	Casting	1.2
			Cu	Casting +MTT	0.12–0.15
			Cu	Casting +MTT	0.4-0.7
			Cu+4%Sn	Casting	0.14-0.43
			Cu+11%Sn+1% Pb	Casting	0.14-0.33
			Cu+17%Sn	Casting	1.43-1.91
Kamenka	2400	Sand	Cu+2%Sn	Casting	0.083-0.37
			Cu+25%Sn+4% Pb	Casting	0010-0.013
			Cu+23%Sn+3% Pb	Casting	0.013-0.017
			Cu+6%Sn	Casting+MTT	0.017-0.024

MTT = mechanical thermal treatment (working)

The higher corrosion rate of bronze artefacts from Olbiya than those from Kamenka can be explained by the predominance of organic and carbonaceous carbon, S and Cl, as well as by the presence of minerals of calcite and gypsum, which may promote quicker corrosion of copper and copper alloys when interacting with water. Study of external surface layer corrosion products by X ray spectral method revealed that Cl, C, Fe, Al, and Pb present in the surface layer point to the processes of interaction of metal with the environment. X ray phase analysis of corrosion products of copper and bronze artefacts from Olbiya also revealed copper combinations with other elements present in soil in the corrosion products: $CuCl_23Cu[OH]_2$, $CuClO_4$, $Cu,Fe)_3Fe_6[PO_4]_4[OH]_{12}$, $CuCa[AsO_4][OH]$.

7. CONCLUSIONS

Although the geochemical environment of the sites were different, in particular, more oxidizing than anticipated in geological repositories, the results of this study are relevant to the subject of geological disposal. It can be used for scoping the boundaries of predicted performance of the waste package in geological repositories and in building confidence in the safety assessment results.

The glass samples, that were taken from archaeological monuments of the Ukraine, were found to be related to the silicate glass type. Our study showed that, under hydration conditions, a superficial layer of complicated structure was formed on the glass surface. This superficial layer was highly porous, with the “specific surface” in the range ~200 m^2/g. This layer probably served as a geochemical barrier for components of glass leaching. It was also established that the overall rate of glass alteration was primarily controlled by the local physical/chemical conditions of the surrounding soil.

The corrosion rate of copper and bronze artefacts also depended on the geochemical conditions of the environment. The Olbiya soil exhibited more aggressive geochemical properties, which, correspondingly, promoted a higher corrosion rate of pure copper and/or bronzes than the soils of the Kamenka site. It appears that the dominating factors that accelerated the corrosion process were the presence of organic matter, S and Cl, and also the presence of calcite and gypsum minerals dissolved in water.

Another important factor determining the corrosion susceptibility of copper and copper-based alloys was the structural state of the metal, which depended on the chemical composition, technological features of moulding and subsequent mechanical-thermal treatment in the course of manufacturing of the artefacts. Metallographic analysis revealed that the artefacts manufactured by cold or hot forging were the most corrosion resistant. Among the cast metals, the high-tin bronzes were the most corrosion-resistant, probably due to formation of thin film of oxidative phase on the surface, which served as an inhibitor of further corrosion.

It could be concluded that among the studied ancient anthropogenic analogues of materials that could be used for radioactive waste containers, the most suitable are pure copper and low-tin bronzes (capable of withstanding mechanical-thermal treatment).

ACKNOWLEDGEMENTS

The authors would like to express their gratitude to colleagues in the Ukraine that contributed to the work: Dr. V. Yachmenev for editorial assistance, Dr. V. Krapivina for the opportunity to participate in the field expeditions of the Institute of Archaeology of National Academy of Sciences, and the IAEA for supporting this work under Research Contract No. 10748.

REFERENCES

[1] WERME. L., Design premises for canister for spent nuclear fuel. POSIVA Technical Report, TR-98-08 (1998).

[2] JOHNSON, L.H., TAIT, J.C., SHOESMITH, D.W., CROSTHWAITE J., GRAY, M.N., Atomic Energy of Canada Limited Report, AECL-10718 (1994).

[3] KING, F., Applied Geochemistry, 10, 477 (1995).

[4] KING, F., AHONEN, L., VUORINEN, U., WERME, L., Copper Corrosion under Expected Conditions in a Deep Geologic Repository, Report POSIVA 2002-01 (2002).

[5] GRAKOV, B,N, Kamenka Site of Ancient Settlement on the River Dneper, Archeology, No. 36 (1954).

[6] GAVRILYUK, N.A., History of Steppe Scythia Economics, VI- III Centuries B.C., Kiev (1999).

[7] KRYZHYTSKY, S.D., et.al., Population and Environment in the Antique States of North Prichernomor'e, 66 (1993).

[8] SHILIK, K.K., Concerning Palaeogeoraphy of Olbiya , Olbiya, Kyiv, 51 (1975).

[9] SKRIPKIN, V.V., KOVALYUCH, N.N., Recent Developments in the Procedures Used at the SSCER Laboratory for the Routine Preparation of Lithium Carbide, Radiocarbon, 40, 211 (1998).

[10] ANDERSSON, C.G., Test Manufacturing of Copper Canisters with Cast Inserts, SKB Technical Report, TR-98-09 (1998).

[11] ABRAITIS, P.K., LIVENS, F.R., MONTEITH, J.E., et al., The Kinetics and Mechanisms of Simulated British Magnox Waste Glass Dissolution as a Function of pH, Silicic Acid Activity and Time in Low Temperature Aqueous Systems, Applied Geochemistry 15, 1399 (2000).
[12] TSYMERMAN, R., GUNTER, K., Metallurgy and Material Science, Reference book, Moscow, Metallurgy, 279, 1982.
[13] LEBEDEV, K.P., RAITS, L.S., SHEMETOV, G.F., GORIACHEV, A.D., Cast Bronzes, Machine Industry, 311 (1973).

CONTRIBUTORS TO DRAFTING AND REVIEW

Brush, L.	SANDIA National Laboratory, United States of America
Cabanillas, E.	Comisión Nacional de Energía Atómica, Argentina
Chapman, N.	ARIUS, Switzerland
Chen, Z.	Beijing Research Institute of Uranium geology, China
Kang, Ch.H.	Korea Atomic Energy Research Institute, Republic of Korea
Knapp, M.	International Atomic Energy Agency
Laciok, A.	Nuclear Research Institute, Czech Republic
Manichev, V.	State Scientific Centre of Environmental Radiochemistry, Ukraine
Nachmilner, L.	International Atomic Energy Agency
Palacios, T.A.	Comisión Nacional de Energía Atómica, Argentina
Potier, J.M.	International Atomic Energy Agency
Raynal, M.	International Atomic Energy Agency
Zhou, W.	East China Geological Institute, China
Zlobenko, B.	State Scientific Centre of Environmental Radiochemistry, Ukraine

Research Coordination Meetings

Řež, Czech Republic: 16–20 October 2000
Vienna, Austria: 4–8 March 2002
Beijing, China: 28 June–2 July 2004